UMTRI-94-7

EXPERIMENTAL VALIDATION OF AIRBAG ABRASION TEST PROCEDURE

FINAL REPORT

Matthew P. Reed
Lawrence W. Schneider
Carol C. Flannagan

University of Michigan
Transportation Research Institute
2901 Baxter Road
Ann Arbor, Michigan 48109-2150

Submitted to:

TRW Safety Systems
4051 N. Higley Road
Mesa, AZ 85215

March 1994

Technical Report Documentation Page

1. Report No.	2. Government Accession No.	3. Recipient's Catalog No.
UMTRI-94-7		

4. Title and Subtitle	5. Report Date
EXPERIMENTAL VALIDATION OF AIRBAG ABRASION TEST PROCEDURE	March 1994
	6. Performing Organization Code
7. Author(s)	8. Performing Organization Report No.
Matthew P. Reed, Lawrence W. Schneider, Carol C. Flannagan	UMTRI-94-7
9. Performing Organization Name and Address	10. Work Unit No. (TRAIS)
University of Michigan Transportation Research Institute 2901 Baxter Road Ann Arbor, Michigan 48109	11. Contract or Grant No.
	13. Type of Report and Period Covered
12. Sponsoring Agency Name and Address	FINAL REPORT
TRW Safety Systems 4051 N. Higley Road Mesa, Arizona 85215	14. Sponsoring Agency Code

15. Supplementary Notes

16. Abstract

The validity of a laboratory test procedure for predicting the skin abrasion potential of driver-side airbags was investigated by comparing test results with abrasion injuries resulting from airbag deployment tests with human volunteers. A series of thirty-two airbag deployment tests was conducted using the laboratory test procedure, and a second identical series was conducted using the legs of volunteer subjects. In each series, the tests included deployments with two levels of inflator capacity, distance, module cover retention, airbag fold, and gender. In the volunteer tests, abrasions resulted from all but four deployments. Statistical analyses were conducted to investigate the effects of the test variables on abrasion severity. Abrasions were found to be significantly smaller in area for a deployment distance of 275 mm than for 200 mm. The two folds produced significantly different abrasion severities. Gender and module cover retention did not affect abrasion severity. Results for inflator effect were compromised by a misclassification of airbag modules.

The abrasion prediction procedure is based on measurement of the pressure exerted by the deploying airbag on a rigid target cylinder using pressure-sensitive Prescale film. Previous research had shown a correlation between patterns of peak pressure on the Prescale film and patterns of skin abrasion. In the current study, a correlation between the area of Prescale film exceeding 90 kg/cm^2 and the area of injury was observed in tests with the target surface located 200 mm from the module, but not at 275 mm. This threshold level is substantially lower than the 175-kg/cm^2-threshold level previously proposed. High-speed films of airbag fabric kinematics suggest that skin abrasion can occur with fabric actions that produce between 90 and 175 kg/cm^2 in the Prescale-film test if lateral fabric motion is present. Guidelines for applying the test procedure using the injury tolerance data obtained in human-subject testing are presented.

17. Key Words	18. Distribution Statement
Airbag, Abrasion, Injury Tolerance, Injury Mechanisms, Skin Injury, Restraint Systems, Biomechanics	Unlimited

19. Security Classif. (of this report)	20. Security Classif. (of this page)	21. No. of Pages	22. Price
None	None	76	

ACKNOWLEDGMENTS

This research was sponsored by TRW/VSSI. The authors extend their thanks to Donna Trojan, Rick Gilbert, and Steven Peterson of TRW for their guidance during the project. Thanks also to Brian Eby and Stewart Simonette of UMTRI's Biosciences Division for technical support, and to Lynn Langenderfer for assistance with subject testing. Special recognition is due to the men and women who participated in testing, all but two of whom volunteered for a second test after experiencing one deployment. The authors also recognize the contributions of Richard E. Burney, M.D., who provided medical support to the project.

CONTENTS

LIST OF TABLES

LIST OF FIGURES

1.0 INTRODUCTION

Driver-side airbag systems have been shown to reduce the incidence of severe injuries to the head and chest (Evans 1990; Huelke *et al.* 1992). Safety benefits have been shown for both belted and unbelted drivers. However, injuries caused by airbags have also been reported. Although several drivers positioned in close proximity to the airbag module have sustained serious or fatal injuries apparently due to the airbag deployment, most of the reported airbag-induced injuries have been minor. These injuries have included skin abrasions, first- and second-degree burns, corneal abrasions, and upper extremity lacerations and bone fractures (Huelke *et al.* 1993; Huelke *et al.* 1992; Rimmer and Shuler 1991).

Airbag-induced skin abrasions have been studied in the laboratory using static deployments. Kikuchi *et al.* (1975) produced abrasions in rabbits using a laboratory airbag system driven by compressed gas, and recommended an airbag-fabric impact velocity of not more than 81 m/s to reduce risk of skin abrasion. Comparisons between the Kikuchi *et al.* data and more recent studies are difficult because there are substantial differences between the laboratory airbag system used in the Kikuchi *et al.* study and current airbag systems, particularly with regard to fabric kinematics.

Schneider *et al.* (1991) conducted 48 deployments into the legs of human volunteers to investigate the effects of distance, inflator capacity, airbag fold technique, and airbag tethering on abrasion severity. Distance was found to be an important factor with a U-shaped effect: abrasions were more severe with the subject's leg 225 mm and 350 mm from the module than at intermediate distances. The airbag fold technique strongly influenced the abrasion severity by altering the deployment kinematics. Tethered airbags produced less severe abrasions at distances equal to or greater than the length of the tether. No significant differences in abrasion severity were observed between 840-denier and 420-denier airbag fabric. Two inflators with nominal peak tank pressures of 350 kPa and 475 kPa did not produce significantly different abrasion severities.

Reed *et al.* (1992) conducted similar static deployment tests with different airbag modules. Distance was again found to strongly affect abrasion severity. Untethered airbags demonstrated the U-shaped distance effect found by Schneider *et al.* Tethering was again found to reduce abrasion severity at distances greater than or equal to the length of the tether by restricting the volume of the deployment envelope in which fabric-skin contact could occur. Airbag modules with 350-kPa inflators produced more severe abrasions than those with 320-kPa inflators. Comparison of airbag fabric velocities with injury data suggested that reducing fabric-skin contact velocity below 85 m/s would be likely to reduce or eliminate abrasion. Tests with an instrumented leg form and pressure-sensitive Fuji Prescale film showed that the patterns of peak pressure exerted on a rigid test surface matched closely the patterns of abrasion produced in deployments with human legs in identical test configurations.

These findings gave rise to an experimental test procedure to predict airbag abrasion potential documented in Reed and Schneider (1993). The experimental airbag abrasion test procedure was based on data in Reed *et al.* (1992) which indicated that the primary mechanism of airbag-induced skin abrasion was high-velocity, normally directed impact of airbag fabric with the skin. Lateral fabric motion along the skin (scraping) was not found to cause abrasion except in cases where the normal force was also high, which occurred only at sites of high-velocity fabric impact. Subjective comparisons between injury and Prescale-film data at four different test conditions suggested that abrasion occurred in areas of the deployment envelope where the pressure recorded with the Prescale film exceeded 175 kg/cm^2.

The current research was conducted to examine the validity of the experimental abrasion-prediction test procedure and the preliminary pressure threshold of 175 kg/cm^2. In addition, the effects of several airbag design and deployment factors on abrasion severity were examined. This research was carried out by conducting two series of airbag deployments based on a statistically powerful experimental design. In one series, airbags were deployed into the legs of volunteer subjects. In the second series, deployments were conducted with the Prescale-film procedure under the same test conditions used in the first series.

This report describes the test methodology, analysis procedures, and results of this research. Conclusions are drawn regarding the effectiveness of the experimental test procedure for predicting airbag-induced skin abrasion, and guidelines are presented for its use.

2.0 METHODS

Test procedures used in this research are based on methods previously documented in Reed *et al.* (1992) and Reed and Schneider (1993). The methods for human-subject testing and Prescale-film testing are discussed separately.

2.1 HUMAN SUBJECT TESTING

The primary goal of human-subject testing was to obtain an abrasion-injury database spanning a range of injury severities and produced by known airbag deployment conditions. The database was intended for subsequent comparison to the abrasion predictions obtained by the experimental procedure. Additional information was sought regarding the quantitative effects of several design and deployment factors on abrasion severity.

2.1.1 Selection of Factors

Five airbag design and deployment factors were identified for study. Previous research (Schneider *et al.* 1991; Reed *et al.* 1992) indicated that distance, tether, inflator capacity, and fold technique were important determinants of abrasion severity. Distance was selected as a factor in the current study to examine the suitability of the abrasion-prediction procedure for various abrasion types, which are known to vary with distance. Tether was removed from consideration because input from the sponsor indicated that few airbag systems are now being designed without tethers.

Inflators are frequently characterized by the pressure histories that are produced when they are deployed into a sealed, 1-ft^3 tank. The most commonly cited value is the peak pressure (kPa) produced in the tank, but peak values of the pressure slope (kPa/ms), averaged over a moving 10-ms window, are also reported. The peak pressure is related to the total mass of gas produced by the inflator and the temperature of the gas, while the pressure slope is more closely related to the rate of mass flow. The two parameters are often written together (*e.g.*, 350 x 22 kPa designates a 350 kPa inflator with a peak slope of 22 kPa/ms). The inflator slope was of interest because of evidence from the previous research that the slope might be a better index of the inflator effect on abrasion than the peak pressure. Unfortunately, two inflators with the same peak pressure but substantially different slopes could not be obtained for testing. Instead, two inflators with nominally identical slopes but different peak pressures were used. In previous testing (Reed *et al.* 1992), two inflators that differed in peak pressure by only 30 kPa, but also differed in slope by 5 kPa/ms, produced different abrasion severities. A null result with inflators that differ in peak pressure by 50 kPa but are nominally identical in slope would tend to support the hypothesis that slope is more closely related to abrasion severity than is peak pressure.

Fold technique was selected for consideration because previous research had shown that changes in fold are the most promising engineering approach to reducing airbag abrasions (Schneider *et al.* 1991). Two other factors, Cover and Gender, were added to the matrix to give a total of five factors under consideration. High module cover breakout pressures were believed to increase abrasion severity by increasing the speed of the airbag fabric as it exits the module. Slitting the module cover to reduce the breakout pressure was hypothesized to reduce abrasion severity. Females were found to be slightly less sensitive to airbag-induced skin abrasion than males in Schneider *et al.* (1991). Equal numbers of males and females were tested in the current study to investigate this effect.

Table 1 shows the test factors and the *a priori* hypotheses regarding their effects on abrasion severity.

2.1.2 Test Matrix

Although 32 human-subject tests were planned, a fractional factorial experimental design with $n = 2$ in each cell was chosen rather than a full-factorial design to allow for direct estimation of repeatability and intersubject variance. Table 2 shows the test matrix. The test conditions were numbered 1 through 32, with conditions 1 through 16 equivalent to

TABLE 1
Design and Deployment Factors Investigated In Human-Subject Testing

Factor and Levels	*A Priori* Hypotheses
Distance 200 mm 275 mm	In previous research, 225 mm and 300 mm were found to be appropriate distances for testing two different patterns of abrasion. Because the airbags in this study were slightly smaller in diameter, these distances were each decreased by 25 mm for this study. As in previous research, injuries were expected to be less severe at the longer distance.
Fold A Fold B Fold	Previous investigations (Schneider *et al.* 1991) suggested that airbag fold technique might affect abrasion severity. Two fold techniques were selected for the current study. The A fold is a fairly typical accordion-style fold. The B fold is a modified accordion-style fold that produces different fabric kinematics.
Inflator 350 x 22 kPa 400 x 22 kPa	The two inflators chosen had nominally identical slopes but different peak pressures in tank tests. Since the difference in fabric impact velocity and abrasion severity was believed to be related more strongly to slope rather than to peak pressure, a null result was anticipated for this factor.
Cover Unslit Slit	In a previous study (Reed *et al.* 1992), abrasions were found to occur primarily when the gage pressure in the airbag was negative, immediately following module cover rupture. Slitting the module cover along the tear seams to reduce the breakout force was hypothesized to reduce the buildup of pressure prior to cover rupture and thereby reduce the velocity of the airbag fabric and subsequent injury severity.
Gender Female Male	In a previous study (Schneider *et al.* 1991), comparable tests with male and female subjects suggested that female leg skin might be less sensitive to airbag-induced abrasion than male skin. A similar result was anticipated in these tests.

conditions 17 through 32. In Table 2, the actual test numbers are listed after the test condition number (*e.g.*, 1-93023 indicates condition 1, test number 93023). The subject numbers are matched with trial numbers and test conditions. For example, test condition 2 (test number 93035) was conducted with subject 5, while test condition 18 (test number 93038), a nominally identical test, was conducted with subject number 6.

The half-fraction of the full factorial was chosen using the values of the five-way interaction among the test factors. One-half of the resulting design was blocked for *homogeneous* test conditions in which the two tests at each condition were conducted with the same subject. In the complementary *heterogeneous* block, the two tests at each condition were conducted on different subjects. The homogeneous/heterogeneous blocks were constructed according to the level of the Cover*Gender interaction. (Because of aliasing inherent in the fractional factorial design, the Cover*Gender interaction is indistinguishable from the Distance*Fold*Inflator interaction.) Tests in the homogeneous block area are shown in gray in Table 2.

TABLE 2
Human-Subject Test Matrix

Test Condition - Test Number		Factor Levels					Subject Number	
Trial 1	Trial 2	Cover	Fold	Inflator	Distance	Gender	Trial 1	Trial 2
1-93023	17-93024	Slit	B*	Low	Low	F	1	1
2-93035	18-93038	No Slit	B	Low	Low	F	5	6
3-93037	19-93040	No Slit	A	High	Low	F	6	7
4-93025	20-93026	Slit	B	High	Low	F	2	2
5-93039	21-93047	No Slit	B*	Low	High	F	7	8
6-93027	22-93028	Slit	B	Low	High	F	3	3
7-93029	23-93030	Slit	A	High	High	F	4	4
8-93048	24-93036	No Slit	B	High	High	F	8	5
9-93015	25-93016	No Slit	B*	Low	Low	M	9	9
10-93021	26-93041	Slit	B	Low	Low	M	13	14
11-93042	27-93044	Slit	A	High	Low	M	14	15a
12-93032	28-93031	No Slit	B	High	Low	M	10	10
13-93043	29-93045	Slit	B*	Low	High	M	15	16
14-93019	30-93020	No Slit	B	Low	High	M	11	11
15-93033	31-93034	No Slit	A	High	High	M	12	12
16-93046	32-93022	Slit	B	High	High	M	16	13

* Asterisks indicate modules that were intended to have A folds that were instead supplied with B folds. See text for details.

The purpose of the homogeneous/heterogeneous blocking was to allow a comparison of between-subjects variance with overall test variance (see Results section for details). All of the original 16 subjects except one (Subject 15) participated in two deployments as called for by the test matrix. Since the subject who declined to participate in the second deployment was a member of the heterogeneous block, another subject could be substituted without compromising the test design. The replacement subject is designated 15a in Table 2. After testing was completed, the airbags with low-capacity inflators that were intended to have A folds were found to have been assembled with B folds, shown as B* in Table 2. (See Section 3.1 for additional explanation.)

2.1.3 Human-Subject Test Procedures

Testing with human subjects followed procedures developed in the previous research (Schneider *et al.* 1991; Reed *et al.* 1992). When the subject reported for testing, he or she was thoroughly briefed on the nature of the research and told that skin abrasions and acute pain immediately following the deployments were likely. Informed consent was obtained in writing.* The legs of male subjects were shaved with an electric razor. The legs of each subject were examined for recent injuries that might affect their sensitivity to abrasion or that could be mistaken for airbag-induced injuries. In no case was the skin condition unsuitable for testing.

The appropriate airbag module was prepared and placed in a steering wheel mounted vertically on the test buck as shown in Figure 1. The steering wheel was rotated 180 degrees from the neutral orientation (to an upside down orientation) because the modules used in testing produce an asymmetrical fabric motion early in the deployment. Mounting the wheel turned 180° directed the predominant fabric motion in the early phases of the deployment toward the wider proximal area of the subject's leg. The subject's leg was positioned vertically in front of the airbag module as shown in Figure 1. The distance between the front surface of the airbag module and the subject's leg was set along the axis of the steering wheel, and a fiduciary mark was placed on the subject's leg at the point of measurement. The subject was provided with hearing protectors and safety glasses. The airbag was deployed while a side-view NAC E-10 camera recorded the airbag kinematics at a nominal 3000 frames per second. A ventilation system with ducts located close to the airbag exhaust ports was activated immediately prior to airbag deployment to remove inflation gases from the laboratory.

Immediately after the deployment, the subject placed his or her leg in a photo fixture for documentation of the injuries. Color photographs were taken 1, 5, 15, and 30 minutes after the deployment. Following the 15-minute photograph, a tracing of the injury was made on a plastic transparency. The transparency was placed over the subject's leg and a fiduciary mark was made corresponding to the mark on the subject's leg to aid in

---

* The rights, welfare, and informed consent of the volunteer subjects who participated in this study were observed under guidelines established by the U.S. Department of Health, Education, and Welfare (now Health and Human Services) on Protection of Human Subjects and accomplished under medical research design protocol standards approved by the Committee to Review Grants for Clinical Research and Investigation Involving Human Beings, Medical School, The University of Michigan.

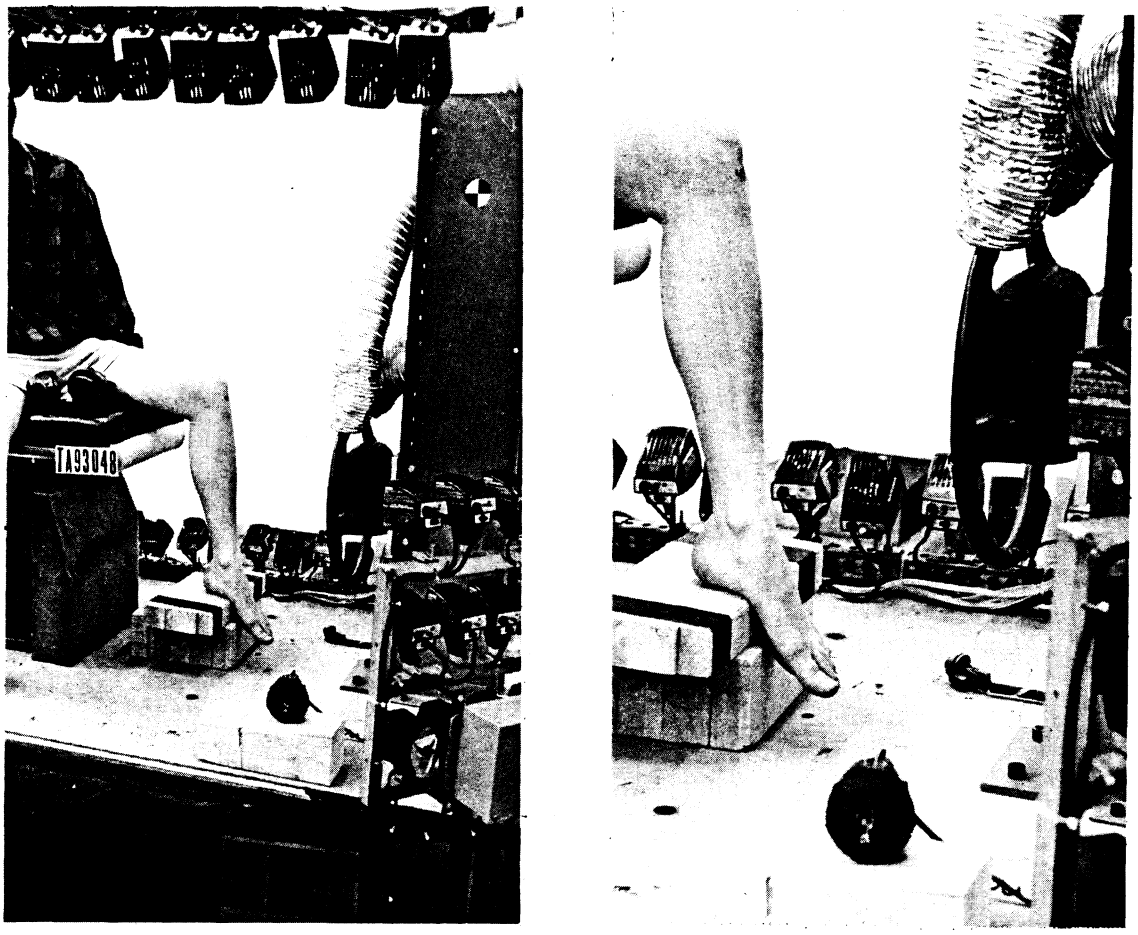

FIGURE 1. Laboratory setup for human-subject testing.

maintaining consistent alignment of the transparency. Markers were used to trace the area of injury onto the transparency. All areas in which the physical integrity of the epidermis was breached, as visible to the investigator without the use of magnifying lenses, were included in the tracing. Large injury areas were outlined while the transparency was held against the subject and filled in after removal. The transparency remained clear over areas of uninjured skin and was opaque in areas of injury. After the photographic sequence was completed, the subject's abrasions were treated with topical hydrogen peroxide and covered with an occlusive dressing. Epidermis was typically regenerated in two weeks.

2.1.4 Analysis of Injury Data

After all human-subject tests were completed, the injury tracings were analyzed digitally. The tracings were scanned at 75 dpi (dots per inch) in 8-bit grayscale mode on a Microtek 600Z scanner and Apple Macintosh computer using Adobe Photoshop software. The fiduciary marks and test numbers written on the transparency were removed in software prior to analysis. The images were converted to bitmap (black and white) with black regions corresponding to the injured area and white elsewhere. The area of injury was computed from the number of pixels that were black.

Statistical analyses using the area of injury as the dependent measure were conducted using JMP software (SAS Institute 1993) on an Apple Macintosh computer. Analysis of variance (ANOVA) was the primary statistical methodology. Preliminary examination of the data showed that the normality assumptions inherent in conventional ANOVA were better met when the injury area data were transformed by taking the square root. Consequently, analyses of injury data presented in this report are based on the square root of the injury area, expressed in millimeters.

2.2 PRESCALE FILM TESTING

2.2.1 Prescale Film Procedures

The experimental abrasion-prediction test procedure uses Fuji Prescale film to record the peak pressure applied by the airbag fabric to the target surface. Fuji Prescale is a plastic film coated with microcapsules embedded in a layer of phenolic resin. The microcapsules contain a color-forming material that reacts with a developer chemical when the microcapsules are ruptured to produce a color change. The film changes from light pink to deep red as the applied pressure is increased. When exposed to time-varying pressure, Prescale-film records the highest pressure applied. Prescale film is available from the manufacturer in several different sensitivities. The film used in this testing is single-sheet, medium-sensitivity film with an effective pressure range from about 50 to 500 kg/cm^2 (700 to 7000 psi).

The test conditions in the human-subject test matrix were duplicated with Prescale film for a total of 32 tests. The laboratory test fixture described in Reed and Schneider (1993) and shown in Figure 2 was used. A piece of Prescale film approximately 360 x 170 mm was fastened to a 100-mm-diameter PVC cylinder with adhesive tape. The airbag to be tested was mounted in the steering wheel and the cylinder-to-wheel distance adjusted to the appropriate test condition. The airbag was deployed, producing an image on the film corresponding to the pattern of peak pressure exerted by the airbag fabric on the target surface. After testing, the film was removed from the cylinder for analysis.

2.2.2 Analysis of Prescale Film Images

The Prescale images were scanned with the same computer hardware used to scan the injury tracings. The images were recorded at 75 dpi in 8-bit grayscale. Image analysis was performed on Macintosh computers using NIH Image software (Rasband 1993) and custom macros written for this application. Preliminary examinations of the Prescale film and injury data indicated that using data from the entire 360 x 170 mm piece of film would be inappropriate when comparing injury areas with pressure patterns, because the area of skin exposed to the airbag was smaller than the Prescale film. Consequently, an area 75 x 150 mm centered horizontally and offset toward the top of the film image was selected for analysis. Figure 3 shows the location of the analysis region within the entire film image. Most of the skin injuries were located in the corresponding areas of the subjects' legs.

In previous testing (Reed *et al.* 1992), a calibration of the Prescale film using 1-ms-duration pressure pulses was obtained with a specially designed apparatus (Reed and Schneider 1993). The calibration curve relates the intensity of the color change in the film to the magnitude of the peak applied pressure. Software changes since the earlier research, and use of a different lot of Prescale film, made an adjustment of the previous calibration curve necessary. The procedure described here is recommended to apply the calibration curve used in Reed and Schneider (1993) to future research of this type.

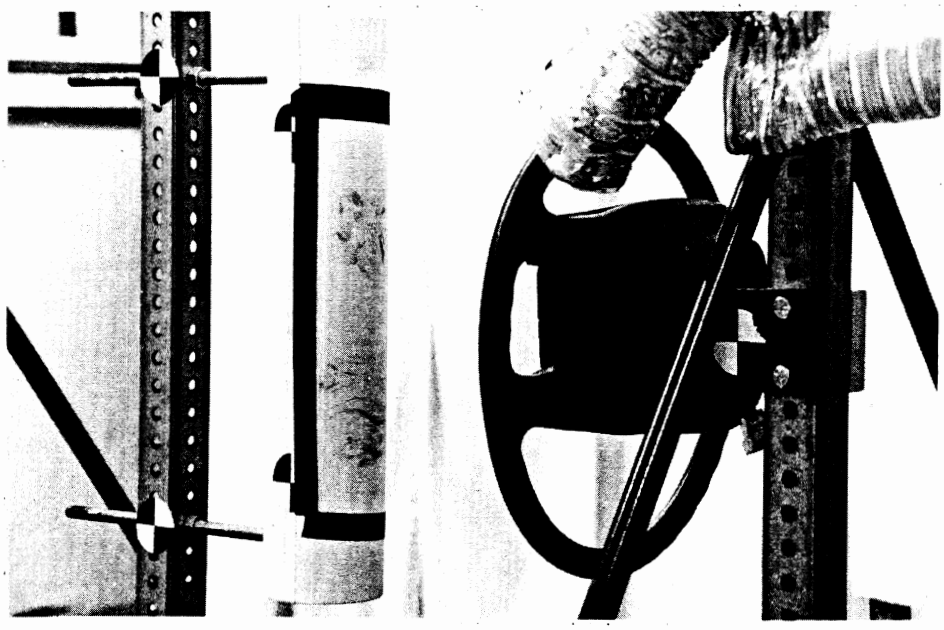

FIGURE 2. Prescale film attached to test fixture.

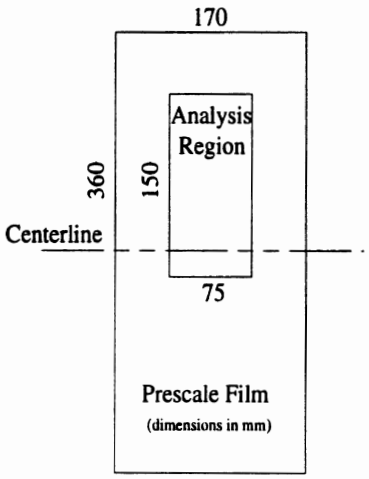

FIGURE 3. Location of analysis region of Prescale-film image.

The original calibration data can be modeled by the polynomial

$$P = -255.4 + 16.79*x - 0.338*x^2 + 3.45E\text{–}3*x^3 - 1.70E\text{-}5*x^4 + 3.33E\text{–}8*x^5 \quad (1)$$

where P is the pressure value in kg/cm^2, and x is the pixel value (0 to 256). Differences in test conditions (*e.g.*, temperature and humidity), Prescale-film lots, scanning hardware, or image-processing software can result in a different relationship between the applied pressure and the resulting pixel value. Temperature and humidity deviations from the conditions used in preparing the calibration can result in a different relationship between applied pressure and color change. The calibration and testing reported here were conducted at 20 ± 2 degrees C. The humidity was not controlled or measured.

A scaling procedure can be used to make an approximate correction for differences due to the Prescale film or scanning equipment. The underlying assumption is that the shape of the calibration curve (the relationship between pressure and pixel value) remains the same even if the overall sensitivity of the film or equipment changes. Thus, only the pixel-value axis is scaled.

In the original calibration trials, maximum pixel values of about 200 were obtained when the film was "saturated," meaning that the maximum color density was achieved. The scaling is performed by measuring the maximum and minimum color density of the film at the time of testing and adjusting the maximum and minimum of the calibration curve to match. The parameter x_c is substituted for x in (1), where

$$x_c = \frac{200\,x}{(PV_{max} - PV_{min})} + PV_{min}, \quad (2)$$

x_c is the scaled pixel value, x is the pixel value obtained in the current testing, PV_{max} is the average pixel value from a saturated area of the film, and PV_{min} is the average pixel value obtained for unexposed film.

The results of this transformation are illustrated here using data from the current testing. The PV_{max} and PV_{min} values were determined by creating saturated areas on an unexposed piece of Prescale film by placing the film against a hard, flat surface and rubbing the plastic (noncoated) side with a steel rod having a 5-mm spherical radius at the end. A person pressing down firmly with such a rod or similar tool can readily saturate the film by rubbing repeatedly over an area. Five 1- to 2-cm^2 areas were saturated to allow comparison of multiple readings. The sample of film was scanned in the same manner as the images from airbag testing. NIH Image software was used to obtain mean pixel values from the saturated areas as well as the adjacent unexposed film areas. Data from five areas were averaged to obtain PV_{max} and PV_{min}. In the current testing, $PV_{max} = 185$ and $PV_{min} = 0$. Equations (1) and (2) were used to obtain a scaled calibration curve, shown in Figure 4 along with the original calibration curve and data. For simplicity, analyses in the Results section of this report are presented using pixel values rather than scaled pressure values. The pixel values are converted to pressure values using the scaled calibration curve illustrated in Figure 4 to compare with previous results and to present recommendations for applying these procedures to other laboratory investigations.

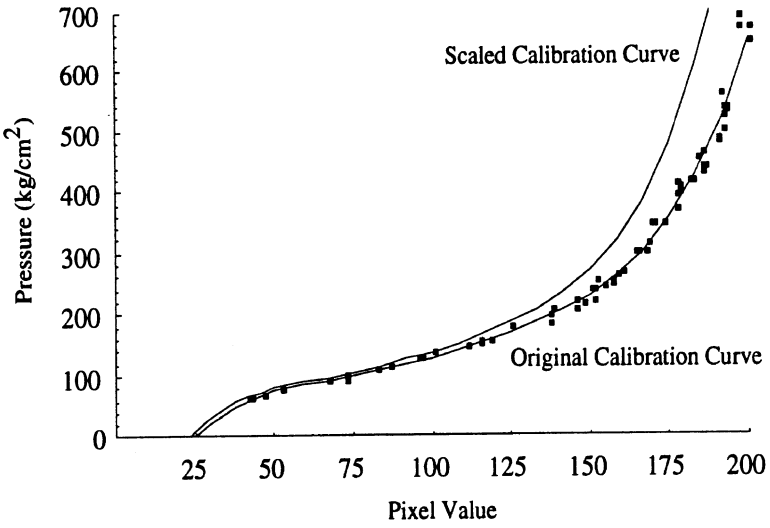

FIGURE 4. Original and scaled (current) calibration curves.

3.0 RESULTS

3.1 RECLASSIFICATION OF TEST CONDITIONS

As the injury data were analyzed, unexpected results concerning an interaction between Fold and Inflator prompted a review of the specifications of the airbag modules that were tested. Airbag modules that were thought to contain the low-capacity (350 x 22 kPa) inflator and A fold were found to have instead been assembled with the B fold. Thus, all test conditions with the 350-kPa inflator included the B fold. There were, however, differences in the abrasion severities produced by airbags with 350-kPa inflators originally thought to contain the A fold and those intended to contain the B fold. Further investigation indicated that the inflators used in the two categories were from different lots, and that performance differences between the lots might account for the difference in injury severity. Because of uncertainty concerning the actual configuration of the nominally 350-kPa-inflator/A-fold airbags, data collected using those airbags were excluded from analyses of factor effects, except where noted. The data were included in comparisons between injury and Prescale-film results, since those analyses required only that the airbags tested with human subjects were the same configuration as those used in the corresponding Prescale-film tests.

3.2 EFFECTS OF DESIGN AND DEPLOYMENT FACTORS ON ABRASION SEVERITY

Abrasions were observed in all but four of the human-subject tests. Figure 5 shows a photo of one of the more severe abrasions. Appendix A contains post-test photos of all 32 tests. Overall, the injuries in this study were less severe, both in depth and area, than those in a previous study (Reed *et al.* 1992).

Table 3 shows the injury results for the human-subject tests. The area of injury was computed by the digital procedure described above. The overall mean of the injury area was 364 mm^2. The average square root of injury was 15.7 mm. Because the low-inflator, A-fold trials were not run with the appropriate airbag modules, the planned analysis of variance (ANOVA) procedures on the full half-fraction design were not appropriate. However, many of the factor effects could still be investigated in subsets of the data.

The analyses were all conducted with the square root of the injured area as the dependent measure and Cover, Inflator, Fold, Distance, and Gender incorporated when appropriate as independent factors. The square-root transformation was used to improve the normality of the ANOVA residuals. All effects were assumed to be fixed. Type-I error probability less than or equal to 5 percent was termed significant.

In the original, fractionated design, each main effect was confounded with the four-way interaction of the remaining effects, and each two-way interaction was confounded with a three-way interaction. Four-way interactions were assumed *a priori* to be nonexistent. Interactions with Gender were also assumed to be nonexistent, so the interaction containing Gender in each two-way/three-way alias relationship was neglected in the analysis. Because the airbag configurations for some trials were in error, smaller fractions of the design were used for analysis. Alias relationships are considered individually for each analysis. In each case, however, all interactions with Gender were assumed to be negligible.

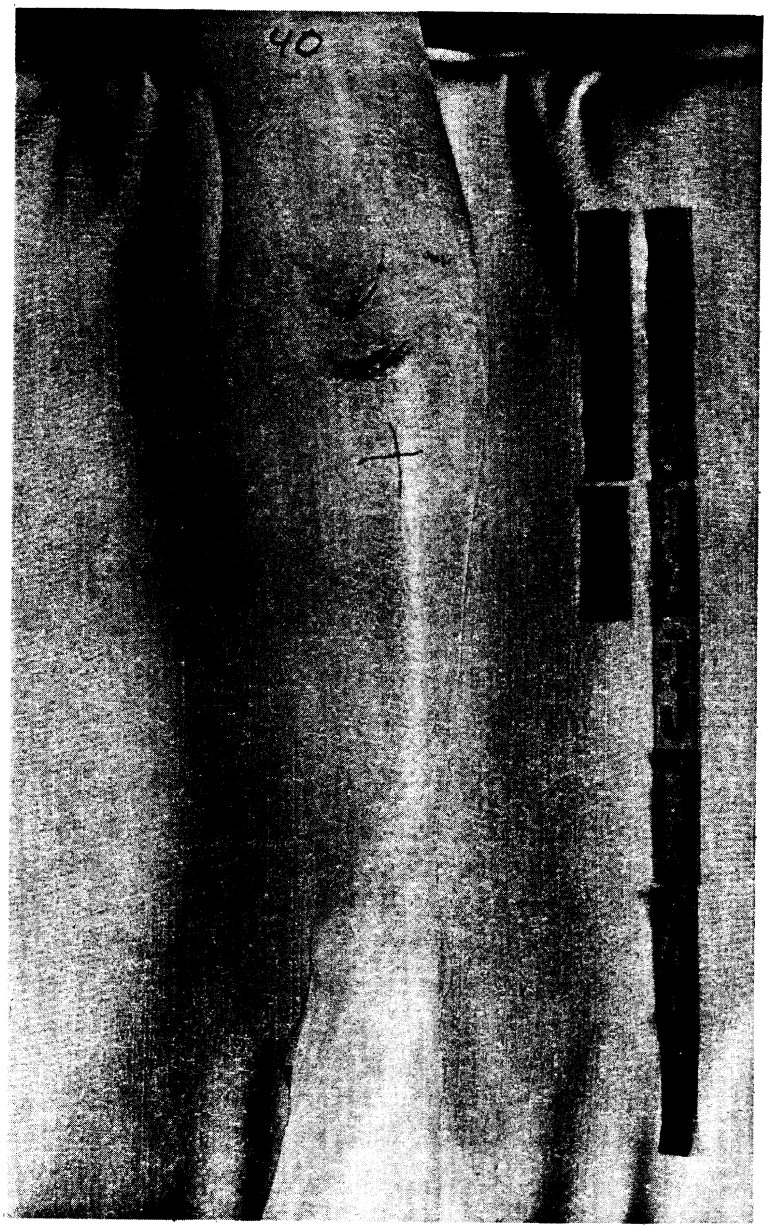

FIGURE 5. Post-test photo of test TA93040, showing an abrasion produced by an airbag with an unslit cover, 400-kPa inflator, A fold, and female subject at 200 mm.

TABLE 3
Injury Results

Test Condition - Test Number		Factor Levels					Injury Area (mm^2)		Square Root of Injury (mm)	
Trial 1	Trial 2	Cover	Fold	Inflator	Distance	Gender	Trial 1	Trial 2	Trial 1	Trial 2
1-93023	17-93024	Slit	B*	Low	Low	F	130.6	285.5	11.4	16.9
2-93035	18-93038	No	B	Low	Low	F	469.4	977.3	21.7	31.3
3-93037	19-93040	No	A	High	Low	F	1466.1	531.3	38.3	23.0
4-93025	20-93026	Slit	B	High	Low	F	244.0	167.2	15.6	12.9
5-93039	21-93047	No	B*	Low	High	F	67.6	362.6	8.2	19.0
6-93027	22-93028	Slit	B	Low	High	F	64.8	0.0	8.1	0.0
7-93029	23-93030	Slit	A	High	High	F	0.0	0.0	0.0	0.0
8-93048	24-93036	No	B	High	High	F	68.9	30.6	8.3	5.5
9-93015	25-93016	No	B*	Low	Low	M	312.5	345.5	17.7	18.6
10-93021	26-93041	Slit	B	Low	Low	M	422.9	1645.0	20.6	40.6
11-93042	27-93044	Slit	A	High	Low	M	1911.2	412.9	43.7	20.3
12-93032	28-93031	No	B	High	Low	M	231.9	290.2	15.2	17.0
13-93043	29-93045	Slit	B*	Low	High	M	109.0	441.2	10.4	21.0
14-93019	30-93020	No	B	Low	High	M	130.1	140.0	11.4	11.8
15-93033	31-93034	No	A	High	High	M	0.0	59.9	0.0	7.7
16-93046	32-93022	Slit	B	High	High	M	249.2	88.5	15.8	9.4

* Asterisks indicate modules that were intended to have A folds that were instead supplied with B folds. Data from these trials are not included in factor-effect analyses, except where noted.

3.2.1 Results from Tests with 400-kPa Inflators

Tests in one-half of the original matrix were conducted with the high-capacity inflator. Selecting only those tests for analysis gives the test conditions and results shown in Table 4. These trials comprise the principal half-fraction of a 2^4 factorial design in Cover, Fold, Distance, and Gender. Each three-way interaction in this design is confounded with a main effect, *e.g.*, the Cover*Fold*Distance interaction is confounded with Gender. All two-way interactions are confounded with other two-way interactions, *e.g.*, Cover*Fold is confounded with Distance*Gender. As noted above, all interactions containing Gender are assumed to be negligible, leaving all main effects except Gender and all two-way interactions clear. The interpretation of the Gender term and its three-way alias is discussed below.

TABLE 4
Injury Results from Tests with 400-kPa Inflators

Test Condition - Test Number		Factor Levels				Injury Area (mm^2)		Square Root of Injury (mm)	
Trial 1	Trial 2	Cover	Fold	Distance	Gender	Trial 1	Trial 2	Trial 1	Trial 2
3-93037	19-93040	No	A	Low	F	1466.1	531.3	38.3	23.0
4-93025	20-93026	Slit	B	Low	F	244.0	167.2	15.6	12.9
7-93029	23-93030	Slit	A	High	F	0.0	0.0	0.0	0.0
8-93048	24-93036	No	B	High	F	68.9	30.6	8.3	5.5
11-93042	27-93044	Slit	A	Low	M	1911.2	412.9	43.7	20.3
12-93032	28-93031	No	B	Low	M	231.9	290.2	15.2	17.0
15-93033	31-93034	No	A	High	M	0.0	59.9	0.0	7.7
16-93046	32-93022	Slit	B	High	M	249.2	88.5	15.8	9.4

Table 5 shows the ANOVA for the injury data from tests with the high-capacity inflator. The two significant effects are shown in **bold**. Distance was the strongest effect. The average square root of the injury area was 23.3 mm at the 200-mm distance and 5.8 mm at the 275-mm distance.

TABLE 5
ANOVA on Square Root of Injury Area for Tests with 400-kPa Inflators

Source	DF	Sum of Squares	F Ratio	Prob>F
Cover	1	0.4556	0.0081	0.9305
Fold	1	69.3056	1.2317	0.2993
Cover*Fold	1	10.0806	0.1792	0.6832
Distance	**1**	**1212.7806**	**21.5541**	**0.0017**
Cover*Distance	1	1.3806	0.0245	0.8794
Fold*Distance	**1**	**574.8006**	**10.2156**	**0.0127**
Gender = Cover*Fold*Distance	1	40.6406	0.7223	0.4201
Error	8	450.135	MSE: 56.267	

The Fold*Distance interaction was also significant. Figure 6 shows the mean values for the two fold levels plotted versus distance. The corresponding data plotted in Figure 7 show that the injury severity for the A-fold was significantly lower at the 275-mm distance than at the 200-mm distance, but the Distance effect was not significant with the B-fold, largely because of one outlier (test no. 93046). The Cover effect (slit versus no slit) was not significant, nor were any two-way interactions with Cover. Since the Gender/Cover*Fold*Distance effect was not significant, there is no need to differentiate between the two confounded effects.

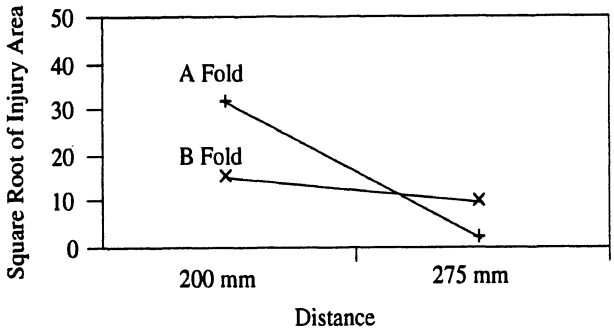

FIGURE 6. Fold*Distance interaction. Mean values are plotted.

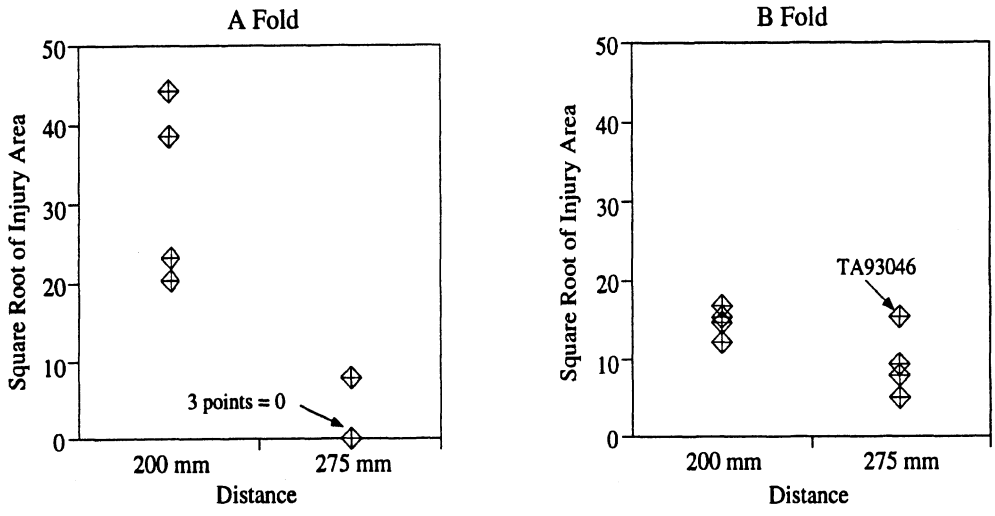

FIGURE 7. Injury data for 400-kPa inflator by fold and distance.
(See text for discussion of test TA93046.)

3.2.2 Comparing Results from 350-kPa and 400-kPa Inflators with B Folds

A test for an Inflator effect can be conducted by analyzing only those tests conducted with B folds as intended (one-half of the test matrix). The alias structure in this design is similar to that described above for the other quarter-fractions of the full design. Table 6 shows the ANOVA results. The main Inflator effect is approaching significance and the Inflator*Distance interaction is significant. Figure 8 shows the effect with mean values.

TABLE 6
ANOVA on Square Root of Injury Area for Tests Conducted with B Folds

Source	DF	Sum of Squares	F Ratio	Prob>F
Cover	1	0.04000	0.0010	0.9751
Inflator	1	131.10250	3.3983	0.1025
Cover*Inflator	1	13.32250	0.3453	0.5730
Distance	**1**	**683.82250**	**17.7254**	**0.0030**
Cover*Distance	1	4.20250	0.1089	0.7498
Inflator*Distance	**1**	**234.09000**	**6.0678**	**0.0391**
Gender = Cover*Inflator*Distance	1	92.16000	2.3889	0.1608
Error	8	308.63	MSE: 38.579	

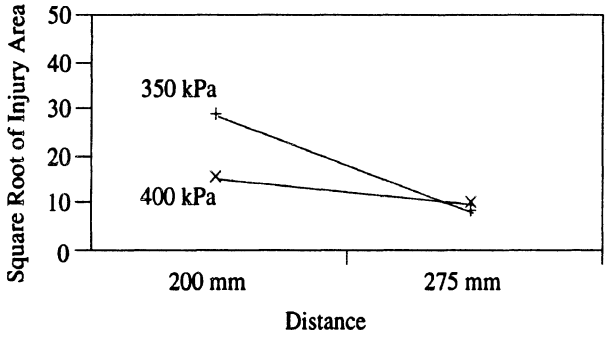

FIGURE 8. Inflator*Distance effect for airbags with B folds.

In the injury data from tests with B folds, there is no difference between the inflators in injury results at 275 mm, but the 350-kPa inflator produced more severe abrasions at the 200-mm distance than the 400-kPa inflator. This effect was contrary to expectations that there would be no inflator effect, or, if there were, that the inflator with the higher peak tank pressure would produce more severe abrasions. Figure 9 shows the data for intended-B-fold airbags at the 200-mm distance and also includes data from the airbags with 350-kPa inflators that were mistakenly configured with B folds rather than A-folds (shown with + symbols). At 200 mm, the abrasion data from the original group of 350-kPa-inflator/B-fold airbags are significantly higher than for the 400-kPa inflator with the B fold ($p < 0.05$). However, the abrasion data from the other group of airbags that was found after testing to also have B folds (and 350-kPa inflators from a different lot) were comparable to the 400-kPa-inflator data. These findings suggest that this apparent Inflator effect is due to differences in the lots of inflators within the range of specification and should be viewed with caution.

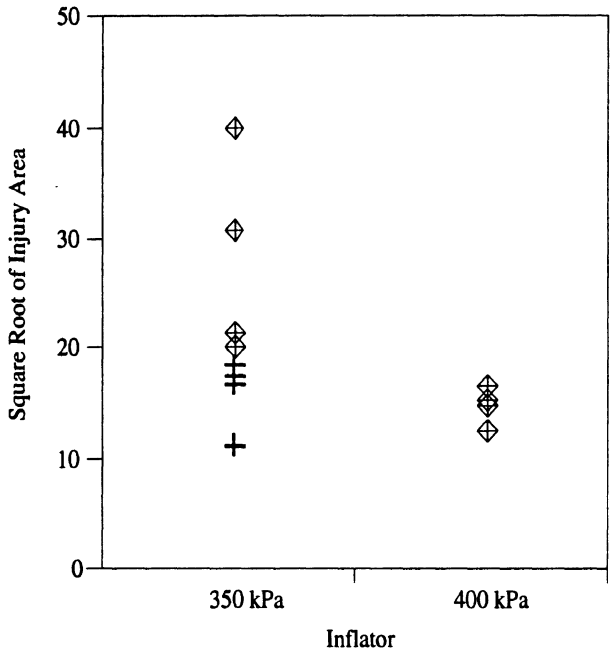

FIGURE 9. Injury data from airbags with B folds at the 200-mm distance. Data from airbags with a different 350-kPa inflator lot are marked with + symbols.

3.2.3 Within- and Between-Subjects Variance

The experimental design included a blocking factor for homogeneous/heterogeneous test conditions to facilitate estimates of within-subject and overall test variance. In tests within the homogeneous block, nominally identical airbags were deployed into both legs of the same subject. In tests within the heterogeneous block, the two duplicate tests were performed with different subjects. The variance observed between homogeneous tests is assumed to result from variability in the test conditions *not* associated with intersubject variations in sensitivity to abrasion, since the same subject participated in both tests. Possible differences in skin sensitivity between an individual subject's legs, or differences due to the tissue geometry of the right and left legs, were neglected. In contrast, the variance between duplicate tests in the heterogeneous block was assumed to result both from intersubject variability in sensitivity to abrasion *and* from the sources of variance also present in the homogeneous block. Thus, the amount of variance due to intersubject differences in skin sensitivity and overall test variance could be estimated.

The mean square error (MSE) is an estimate of test-retest variance or repeatability. The MSE for each block was calculated by dividing the sum of the squared deviations of each observation from the mean for its test condition by the number of degrees of freedom (n = 16 gives 8 df for each block). The square root of the MSE is an estimate of the test-retest standard deviation in the same units as the response variable. Table 7 compares the MSEs and standard deviation estimates between the homogeneous and heterogeneous blocks for both the injury area and the square root of the injury area. The larger variance in the heterogeneous block indicates substantial intersubject variability in sensitivity to abrasion. Since the homogeneous block variance estimate contains all of the same

sources of variance as the heterogeneous block except for intersubject variability, an estimate of the variance due solely to intersubject variability can be obtained by subtraction. For the square root of injury area, the standard deviation due to intersubject variability is about 9.3 mm.

TABLE 7
Estimates of Variance Due to Intersubject Differences and Other Causes

Block	Square root of Injury Area		Injury Area	
	MSE	Std. Dev. (mm)	MSE	Std. Dev. (mm^2)
Homogeneous (test variance *not* due to intersubject differences)	10.4	3.2	2641.58	51.4
Heterogeneous (test variance due to intersubject differences plus that due to other causes)	97.0	9.85	318432	564
Estimate of Variance Due to Intersubject Differences (Heterogeneous minus Homogeneous)	86.6	9.3*	315790	562.*
All tests (test-retest variance for all 16 test conditions)	53.7	7.3	160537	400.7

* Note that the estimates of the standard deviation due to intersubject differences are calculated by the formula $\sqrt{s^2_{hetero} - s^2_{homo}}$, which is not equal to $\sqrt{s^2_{hetero}} - \sqrt{s^2_{homo}}$.

3.3 RESULTS OF TESTING WITH PRESCALE FILM

Pressures exerted by the airbag fabric on the Prescale film were sufficient in all tests to cause a color change in the film. Appendix B contains the digital scans of the Prescale images. Prescale-film analyses were performed using threshold levels expressed in pixel values rather than calibrated (pressure) values. For each test, the area of the Prescale image where pixel values exceeded a threshold level was calculated. Thresholded areas were calculated for pixel values ranging from 10 to 150 in increments of 10 (0 is lightest, 255 is darkest). Only very small areas (*i.e.*, less than 1 mm^2 per scan) were observed at pixel values greater than 100, so only data from thresholds below 100 were used in analyses. As with the injury data, the Prescale data were analyzed after a square-root transformation was applied to reduce the leverage of a few high data values and to increase the normality of the ANOVA residuals. The thresholded area data are reported as Prescale(*nn*), where *nn* is the threshold pixel value. The units of Prescale(*nn*) values are millimeters, rounded to the nearest 0.1 millimeter.

3.3.1 Correlations Among Prescale Data Over a Range of Threshold Values

There was considerable correlation between the thresholded areas calculated at different pixel levels. Table 8 shows the Pearson correlation coefficients (r) for the 32 trials of the Prescale test series for threshold levels from 50 to 90. Prescale(100) assumes values between 0 and 2 and is poorly correlated with lower-threshold data.

TABLE 8
Correlation Coefficients Among Prescale Data Calculated for a Range of Threshold Levels

Variable	Prescale(50)	Prescale(60)	Prescale(70)	Prescale(80)	Prescale(90)
Prescale(50)	1.0000	--	--	--	--
Prescale(60)	0.9883	1.0000	--	--	--
Prescale(70)	0.9497	0.9853	1.0000	--	--
Prescale(80)	0.8734	0.9282	0.9741	1.0000	--
Prescale(90)	0.7420	0.7929	0.8512	0.9165	1.0000

One way to select a threshold value that produces results similar to the injury data is to compare the average square root of injury area with the average Prescale(*nn*) value for each threshold level. Table 9 shows this comparison. The average square root of injury area falls very close to the mean of Prescale(60), suggesting that a threshold level near 60 might provide the best prediction of injury area.

TABLE 9
Comparison of Average Square Root of Injury Area with Average Prescale(*nn*)

Average Square Root of Injury Area (mm)	Average Prescale(50)	Average Prescale(60)	Average Prescale(70)	Average Prescale(80)	Average Prescale(90)
15.7	21.2	15.2	10.0	5.3	1.5

3.3.2 Factor Effects in Prescale Film Data

Since the Prescale-film technique was expected to predict skin abrasion, the same factor effects observed in the injury data were expected in the Prescale data. To investigate this hypothesis, an ANOVA similar to that performed with the injury data was performed with the Prescale(50), Prescale(60), and Prescale(70) data. The analysis was confined to data from tests with 400-kPa inflators. Tables 10, 11, and 12 show the ANOVA results. Gender and Inflator effects are not estimable in these analyses.

Two effects, Fold and the Fold*Distance interaction, are significant for Prescale(50), Prescale(60), and Prescale(70). Prescale(50) data are used to illustrate these effects. Figure 10 shows the Fold*Distance interaction, in which the Fold effect can also be seen. The Prescale(60) Fold*Distance interaction is similar to the interaction in the injury data, except that there is no Distance effect in the Prescale(60) data. The average Prescale(60) value at 275 mm is approximately the same as the average value at 200 mm. This is in sharp contrast to the injury data, which show a strong Distance effect. The Fold effect at 200 mm is about the same magnitude in both Prescale(60) and square root of injury area.

TABLE 10
ANOVA for Prescale(50) Using Data for 400-kPa Inflators

Source	DF	Sum of Squares	F Ratio	Prob>F
Cover	1	26.26562	1.1305	0.3187
Fold	**1**	**695.64062**	**29.9401**	**0.0006**
Cover*Fold	1	18.27562	0.7866	0.4010
Distance	1	7.15562	0.3080	0.5941
Cover*Distance	1	2.48062	0.1068	0.7522
Fold*Distance	**1**	**221.26563**	**9.5232**	**0.0150**
Cover*Fold*Distance	1	14.25063	0.6133	0.4561

TABLE 11
ANOVA for Prescale(60) Using Data for 400-kPa Inflators

Source	DF	Sum of Squares	F Ratio	Prob>F
Cover	1	1.56250	0.0798	0.7847
Fold	**1**	**436.81000**	**22.3090**	**0.0015**
Cover*Fold	1	18.06250	0.9225	0.3649
Distance	1	6.25000	0.3192	0.5876
Cover*Distance	1	2.40250	0.1227	0.7352
Fold*Distance	**1**	**196.00000**	**10.0102**	**0.0133**
Cover*Fold*Distance	1	3.80250	0.1942	0.6711

TABLE 12
ANOVA for Prescale(70) Using Data for 400-kPa Inflators

Source	DF	Sum of Squares	F Ratio	Prob>F
Cover	1	2.32563	0.1500	0.7086
Fold	**1**	**206.64062**	**13.3322**	**0.0065**
Cover*Fold	1	12.78063	0.8246	0.3904
Distance	1	7.70063	0.4968	0.5009
Cover*Distance	1	1.62563	0.1049	0.7544
Fold*Distance	**1**	**139.83063**	**9.0217**	**0.0170**
Cover*Fold*Distance	1	0.27562	0.0178	0.8972

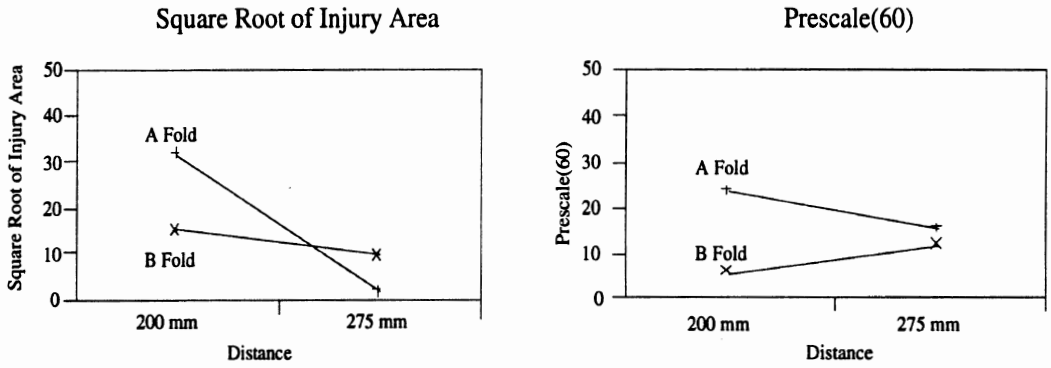

FIGURE 10. Comparison of Fold*Distance interaction in injury and Prescale(60) data for 400-kPa inflators.

3.3.3 Correlation Between Prescale and Injury Data

The relationship between Prescale(60) and the square root of injury area was investigated by linear regression. Means were calculated in both the injury and Prescale(60) data for each of the 16 test conditions. Figure 11 shows a plot of these means. A linear regression fit to the data means (n=16) was not significant. Additional regressions were performed with the data grouped by distance. At 200 mm, the regression approached significance ($p = 0.057$), but the 275-mm regression was not significant. Table 13 shows the regression results. The Prescale procedure predicts the square root of injury area reasonably well at 200 mm ($r = 0.691$), but there is no relationship between the Prescale and injury data at 275 mm ($r = 0.264$).

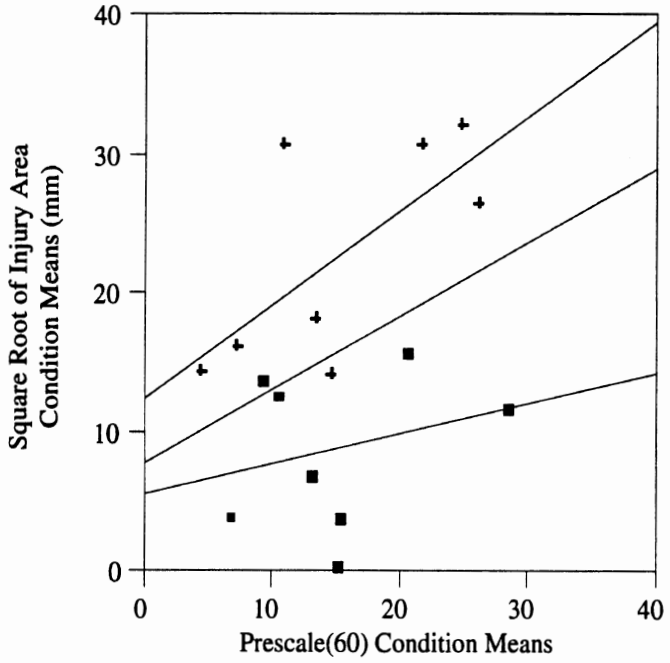

FIGURE 11. Plot of square root of injury area versus Prescale(60) using test condition means (n=16). Data from tests at 200 mm are shown with + symbols. Center line is regression for all test condition means. Upper and lower lines are for regressions for data from 200-mm and 275-mm distances, respectively.

TABLE 13
Regression Results:
Prescale(60) Condition Means versus Square-Root-of-Injury-Area Condition Means

Linear Fit Both Distances
$r^2 = 0.1506$

Source	DF	Sum of Squares	Mean Square	F Ratio	Prob>F
Model	1	221.3114	221.311	2.4825	0.1374
Error	14	1248.0880	89.149		
C Total	15	1469.3994			

Linear Fit Distance=200 mm
$r^2 = 0.4773$

Source	DF	Sum of Squares	Mean Square	F Ratio	Prob>F
Model	1	207.72564	207.726	5.4784	0.0578
Error	6	227.50436	37.917		
C Total	7	435.23000			

Linear Fit Distance=275 mm
$r^2 = 0.0698$

Source	DF	Sum of Squares	Mean Square	F Ratio	Prob>F
Model	1	15.38681	15.3868	0.4501	0.5273
Error	6	205.10694	34.1845		
C Total	7	220.49375			

3.3.4 Test-Retest Variance in Prescale(60) Data

The repetition of each test condition allows an examination of variance similar to that shown in Table 7 for the injury data. The test-retest variance (within test condition) was calculated by averaging the variance estimates for all 16 (2^4) test conditions. For Prescale(60), the variance estimate is 39.1 mm^2 and the estimate of the standard deviation is the square root of 39.1 or 6.3 mm. From Table 7, the test-retest standard deviation for all human-subject tests is 7.3 mm. Thus, the repeatability of the Prescale tests is about the same as the human-subject tests.

However, the Prescale-film test-retest variability would be expected to be better than the variability in the human-subject data because of the added variance in the heterogeneous block due to intersubject differences. From Table 7, the test-retest standard deviation for the homogeneous block is only 3.2. Using only the test conditions in the homogeneous block, the Prescale(60) test-retest standard deviation is 4.8, slightly higher than in the square root of injury area.

The larger-than-expected variance in the Prescale data appears to result from larger values relative to the injury data at the 275-mm distance. The injuries at 275 mm were small, and consequently the test-retest variance estimates were also small because of a floor effect in the data (*i.e.*, no injury area could be below zero). In contrast, no distance effect was observed in the Prescale data, indicating that the average area exceeding the

threshold level was the same at both distances. Since the Prescale data values were larger at 275 mm, there was less of a floor effect, and the test-retest variance estimates were larger.

For both the Prescale and human-subject tests, the test-retest standard deviation is a substantial percentage of the mean data values. For the Prescale(60) data, the ratio is 6.3/15.2 = 41%. For the square root of injury area, the ratio is 7.3/15.7 = 46%, although for the homogeneous block alone the ratio is 3.2/15.7 = 20%. The test-retest standard deviation is also large relative to the standard deviations of the data sets. The standard deviation of the Prescale(60) data across all trials is 8.5, giving a ratio of test-retest-to-total standard deviation of 6.3/8.5 = 74%. For the square root of injury area, the ratio is 7.3/11.1 = 66%. Figure 12 shows these findings graphically. The data points in Figure 12 would form a straight line with unity slope if the tests repeated perfectly. The widths of the data clouds around the diagonals indicates that the poor repeatability of both the human-subject and Prescale tests can be expected to adversely affect attempts to relate the two data sets. Test-retest correlations for both data sets are modest: $r = 0.55$ for the square root of injury area, and $r = 0.48$ for the Prescale(60) data.

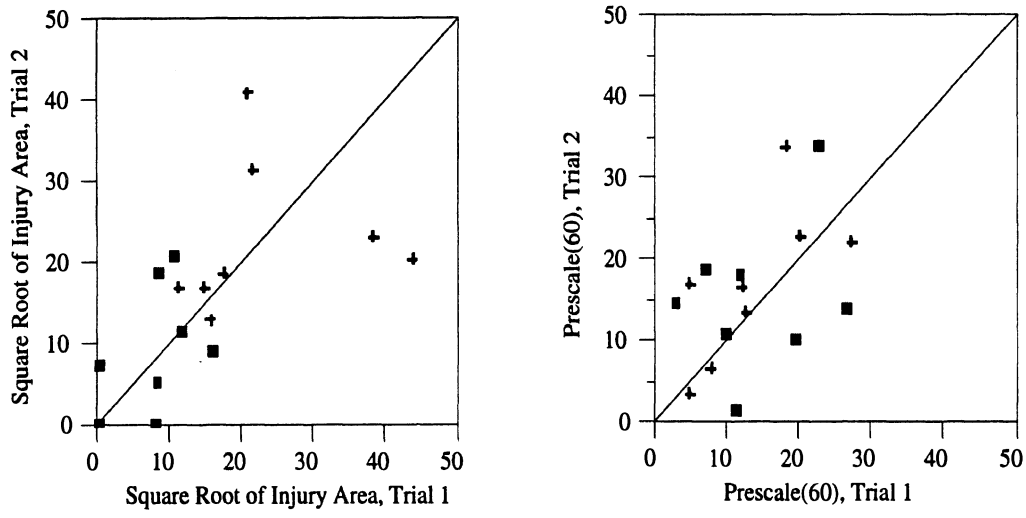

FIGURE 12. Plots of trial one versus trial two for the square root of injury area and Prescale(60). Data from tests at 200 mm are shown with + symbols.

4.0 DISCUSSION

4.1 EFFECTS OF DESIGN AND DEPLOYMENT FACTORS ON ABRASION SEVERITY

The statistical analyses of injury data were hampered by improper configuration of one-quarter of the airbag modules. Instead of a single analysis of the whole design, two separate ANOVAs were conducted on halves of the design that did not include the improperly configured modules. A square-root transformation of the injury area data was used to improve the normality of the ANOVA residuals and to reduce the impact of outliers on the statistical model. The salient ANOVA results are also significant in the injury area data, although the statistical assumptions implicit in ANOVA are better met by the square-root-transformed data.

4.1.1 Distance and Fold

Analyses using only data from tests with 400-kPa inflators showed that abrasions were generally less severe at 275 mm than at 200 mm. There was, however, a significant interaction between Distance and Fold. Abrasions were more severe at 200 mm with the A fold than with the B fold, but at 275 mm there was little difference. With both folds, only one of eight tests at 275 mm exceeded 100 mm^2 (1 cm^2) in injury area, and no abrasion was observed in three tests. Since the overall test-retest standard deviation for injury area was about 400 mm^2, the abrasions at 275 mm with 400-kPa inflators can be considered negligible.

At 200 mm, the average area of abrasion produced by A-fold airbags with 400-kPa inflators was 1080 mm^2 (10.8 cm^2), while the average injury area for B-fold airbags with 400-kPa inflators was only 233 mm^2 (2.33 cm^2). The difference between folds in abrasion severity can be understood by examination of the airbag fabric kinematics. In previous research (Reed *et al.* 1992), severe abrasions were found to occur when high-velocity airbag fabric impacted the skin. In particular, flaps or wings of airbag fabric that swing out of the module as the airbag unfolds reach high velocities and were found to cause abrasions at the point of contact with the skin. Figure 13 shows four frames digitized from high-speed films of deployments with 400-kPa inflators. The four tests shown in Figure 13 were selected for greatest clarity in illustrating the fabric kinematics, but the other tests with the same conditions showed similar kinematics.

At 200 mm, the A-fold airbag shows a typical wing action leading to abrasion. A large flap of airbag fabric swinging upward and toward the subject's leg is the first part of the airbag to contact the skin. Most of the abrasions observed in these tests occurred at the point of initial contact of the fabric with the skin. At 275 mm, the fabric wing has swung past the leg prior to contact. The initial contact with the leg is made by the center part of the airbag moving approximately perpendicular to the leg without substantial lateral motion.

In contrast with the A fold, the B fold produces a rounder airbag shape at the time of contact with the skin at both distances. The upper fabric wing is much smaller, and the center of the airbag contacts the skin first. As noted above, abrasions were smaller with the B fold than with the A fold at 200 mm. Only one test with the B fold at 275 mm produced an abrasion area greater than 1 cm^2 (TA93046, shown in Figure 13). The high-speed film of that test does not clearly show the fabric action responsible for the abrasion, but the overall variability in kinematics between tests suggests that a range of abrasion severities should be expected. At both distances, the B fold performed the same or better than the A fold with respect to abrasion severity.

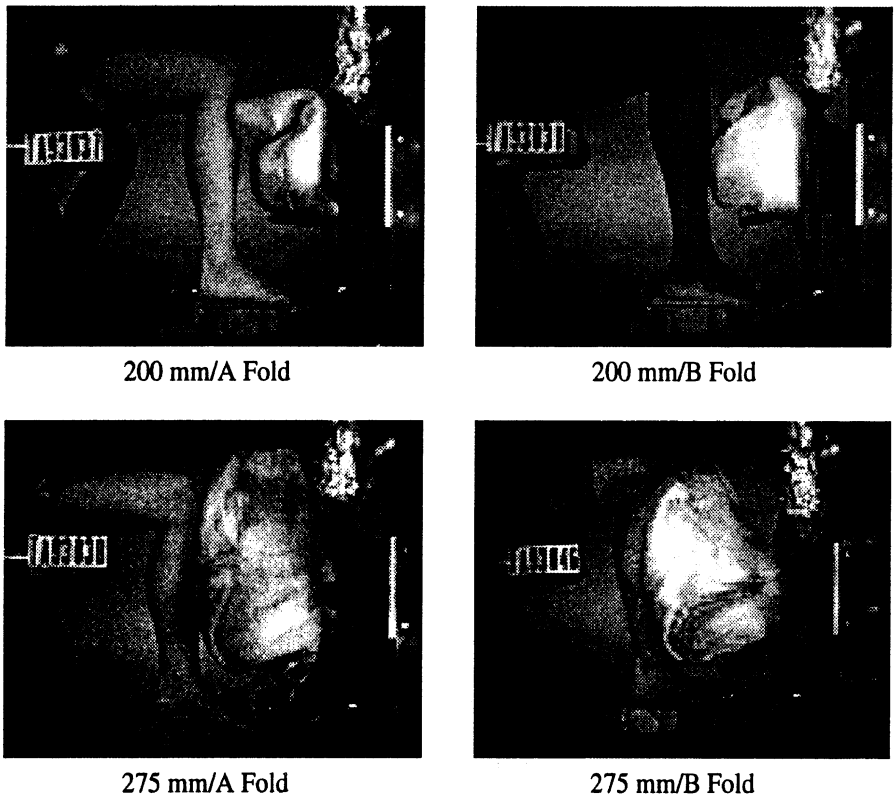

200 mm/A Fold | 200 mm/B Fold

275 mm/A Fold | 275 mm/B Fold

FIGURE 13. Frames from high-speed film of human-subject deployments with 400-kPa inflators, showing fabric kinematics at approximate time of initial fabric-skin contact.

4.1.2 Inflator

A significant Inflator effect was not expected. Although the two inflators had different nominal peak tank pressures, the nominal slopes were identical. Fabric energy responsible for abrasion is believed to be imparted primarily by gas generated before the module cover ruptures. Consequently, the rate of gas production, rather than the total amount generated, is thought to be the more important determinant of abrasion severity. Since one-quarter of the airbag modules were improperly configured, a statistical test of inflator effect could be conducted with confidence on only the original B-fold fraction of the test matrix.

Unexpectedly, the abrasions produced by the 350-kPa inflator at 200 mm were more severe than the abrasions produced by the 400-kPa inflator (see Figure 9), although the Inflator effect was not significant when data from both distances were combined. Since post-test examination showed that the misconfigured airbags also had 350-kPa inflators and B folds, data from those tests were compared with the other tests at 200 mm. This second lot of 350-kPa/B-fold airbags produced abrasions comparable to the 400-kPa inflators. Although there is greater confidence in the configuration of the original B-fold fraction of the test matrix, there is no other justification available for exclusion of the other 350-kPa/B-fold data from consideration. When considered together, the data do not show an inflator effect.

The 350-kPa inflators in the two test groups (those intended to be tested with B folds and those intended to be tested with A folds) came from different lots. Although the lot acceptance-test statistics for the inflators do not show a large difference between the two lots, inflator variance appears to be the most viable explanation for the difference in abrasion severity between the two groups. Other possibilities, including systematic variations in folding procedures, seem unlikely. Overall, assessment of a possible inflator effect is inconclusive, although the results suggest that within-specification variation in inflator output may influence abrasion severity.

4.1.3 Cover and Gender

Cover and Gender did not have significant effects on abrasion severity. The absence of a Cover effect was unexpected, because higher module breakout pressures were thought to result in higher fabric velocities that could produce more severe abrasions. Apparently, the module cover used in this testing had a sufficiently low breakout pressure that the difference between a slit and unslit module cover was not large enough to be significant. This finding has limited generality, because only one module cover was used. Other module covers, with higher breakout pressures, might show significant differences in abrasion severity with slit covers.

Some previous research (Schneider *et al.* 1991) suggested that female skin might, on average, be less sensitive to abrasion. The current research does not support that finding. In each of the ANOVA analyses conducted (400-kPa inflators only and B folds only), the Gender effect was confounded with a three-way interaction, potentially making interpretation difficult. However, in neither case was the effect significant.

4.1.4 Test-Retest Variance

The experimental design allowed discrimination between variance in the injury data due to differences in subject sensitivity to abrasion and due to variability in other aspects of testing. The variation in the dependent measures not due to the controlled factors can be attributed to three sources. Specification error refers to deviations of the actual airbag modules from the nominal values. For example, the airbags used in this testing were folded by hand and some variation in fold can be expected. Procedural error is due to experimenter-controlled factors. In this category, one potentially important source of error is the positioning of the subject's leg prior to testing. The distance from the skin to

the airbag module at points other than along the axis of the steering wheel can vary between tests because of the irregular geometry of the leg. Subject error is variance due to differences in leg geometry, tissue properties, skin sensitivity to abrasion, and other factors intrinsic to the subject. The magnitude of the variance due to these sources was estimated to aid in the design of future experiments.

The homogeneous/heterogeneous subject blocking allows estimation of subject error. The test-retest standard deviation of the square root of injury area was about three times higher between subjects than within subjects, demonstrating substantial intersubject variability in sensitivity to abrasion. These results suggest that a within-subjects design should be used whenever possible in abrasion testing to reduce the influence of intersubject variability. However, since the maximum number of deployments a person can participate in under the current test protocol is two, future testing with human volunteers will often require intersubject comparisons.

The estimates of intersubject variance provided in Table 7 should be considered with some caution because of the influence of two characteristics of the experimental design and data. First, the homogeneous/heterogeneous block was constructed based on the value of the Cover*Gender interaction, which is equivalent to the Fold*Inflator*Distance interaction because of the aliasing inherent in the experimental design. The Fold*Inflator*Distance interaction accounted for a substantial amount of the variance in the data, although the analysis was not performed because of the misclassification of one-quarter of the airbag modules. The result of the alias relationship between the Fold*Inflator*Distance interaction and the subject blocking is that the heterogeneous block has a significantly higher mean response value.

Second, the test-retest variance is correlated with the square root of injury area as a result of the floor effect in the injury data. The correlation coefficient between the test condition means and the difference between Trial 1 and Trial 2 at each test condition is 0.728. Because higher response values are associated with higher test-retest variances, the difference in mean response between the blocks can be expected to *increase* the estimate of intersubject variability.

However, there is another factor that would tend to *reduce* the intersubject variance estimate. About half of the test conditions did not result in substantial abrasions (primarily those at the 275-mm distance), thus producing test-retest variance estimates below those that would be expected if all trials resulted in substantial abrasions. Even with these qualifications, the estimates presented in this report are probably reasonable for predicting the number of tests that will be required to achieve a desired level of statistical confidence.

4.2 PRESCALE FILM AS AN ABRASION PREDICTION TOOL

The primary goal of this research project was to examine, using quantitative analysis techniques, the relationship between airbag-induced skin abrasions and the patterns of peak pressure on a rigid test surface produced under nominally identical test conditions.

The experimental techniques were developed previously (Reed and Schneider 1993). At issue in this research were the analysis and interpretation of results.

The pressure measured on the rigid test-fixture surface by the Prescale film is not necessarily the same as the pressure that would have been sustained by skin at the same location because of the compliance of the skin and underlying tissue. Although previous testing (Reed *et al.* 1992) showed that the pressures on the skin surface were similar to those on the rigid target surface for a small number of comparable tests, an accurate prediction of skin surface pressure is not required. The Prescale-film data are used to predict abrasion, rather than to predict the skin surface pressure. It is sufficient for a correlation to be demonstrated between a Prescale-based measure of airbag fabric action and the incidence of abrasion under similar deployment conditions. For ease of discussion, the Prescale pressures produced by airbag fabric actions that cause abrasion are referred to without reiterating the link between the Prescale data and the actual skin pressure.

4.2.1 Calibration of Prescale Film

Interpretation of a Prescale-film image as a pressure field requires reference to a calibration curve relating the density of the film image to peak applied pressure. In previous research (Reed *et al.* 1992), a calibration curve was developed using 1-ms-duration pressure pulses. Generating that calibration required a specially designed apparatus and a substantial amount of time. The complexity of the calibration process mandated the development of a simpler way of obtaining a useful calibration curve for the current and future research.

The calibration curve developed in the previous research should not be used "as is" because differences in the hardware or software used to scan and analyze the Prescale image can render invalid a calibration curve obtained with other hardware or software. A compromise procedure was adopted for the current project that should be applicable to future research. The assumption underlying this compromise procedure is that the hardware and software used for analysis will, in general, produce an approximately equivalent relationship between the image density and pixel values. Differences are assumed to exist only in the overall "gain" of the system—that is, in the ratio between the pixel values assigned to unexposed and saturated Prescale film. The shape of the calibration curve between 0 and 100 percent of the Prescale film's range is assumed to be constant. The scaled calibration curve is believed to be adequate because the pressure thresholds that have been identified for predicting abrasion are only approximate and more accurate calibration would not substantially improve the prediction.

4.2.2 Selection of a Threshold Level

The injury-prediction measure computed from the Prescale-film images is the area of the film that exceeds a particular pressure level. In this study, pressure levels did not exceed about 100 pixel value, or about 145 kg/cm^2. In the previous study, a level of 175 kg/cm^2 was proposed as the pressure above which abrasion was predicted. Since abrasions were

observed in the current test series, it is clearly possible to produce abrasions with airbag fabric actions that result in pressures less than 175 kg/cm^2 on a rigid target surface.

The selection of a threshold level that would accurately predict the area of abrasion was more difficult than anticipated. First, the large test-retest variance made determining a relationship between injury and the Prescale data difficult. Second, the hypothesized relationship between the Prescale-film images and the patterns of injury appeared to hold only for the 200-mm distance. In view of these complications, the threshold level was chosen as that which produced the mean response over all test conditions closest to the mean of the injury response (the square root of injury area). This threshold was 60 pixel value, or 93 kg/cm^2 using the scaled calibration curve. Prescale analyses using pixel values of 50 or 70 produced similar correlations with injury, so the selection of a threshold value could not be made using that criterion. Although the current calibration curve translates 60 pixel value to 93 kg/cm^2, a threshold level of 90 kg/cm^2 will be used to avoid implying greater precision than is warranted.

The correlation among Prescale data calculated using different threshold levels reflects an important characteristic of the airbag fabric action and Prescale response. With the airbag modules studied, the area of abrasion is much smaller than the total skin area exposed. Similarly, the area of Prescale film that shows a response (*i.e.*, peak pressure greater than the film's lower sensitivity threshold) is also smaller than the total area exposed, although generally larger than the area of injury. For tests at 200 mm, the pattern of the pressure image on the Prescale film is similar to the pattern of injury in the corresponding human-subject tests. At the edges of the injury area, the spatial pressure gradient is steep, meaning that relatively large changes in a pressure threshold value (*e.g.*, from 50 to 60 pixel value) will change the area calculation only slightly and in a consistent way across tests. Consequently, a range of threshold values will produce area calculations that correlate about equally with injury.

4.2.3 Correlation Between Prescale and Injury Data

Primarily because of large test-retest variance and a small range of injury severities, no overall correlation between Prescale(60) and injury was found. Analyses on subgroups of data showed a good correlation in data from tests at 200 mm, but there was no correlation at 275 mm. Since threshold levels were the same at each distance (the square root of the area above the threshold level is the dependent measure), these results suggest that a different injury mechanism was operating at 200 mm and 275 mm.

Previous research (Reed *et al.* 1992) showed that pressures above 175 kg/cm^2 (115 pixel value with the current calibration) could produce injury in the absence of scraping action by the airbag fabric. Two types of experimental evidence led to this finding. First, stamp abrasions were observed with tethered airbags striking the skin surface at the outer edge of the deployment envelope. High-speed film showed that the impacts were normally directed with little or no lateral movement. Abrasions were observed at the point of fabric impact, and Prescale-film tests with identically configured airbags showed pressure greater than 175 kg/cm^2 in the areas of injury. Second, experiments were conducted in which Prescale film was placed over the subject's leg prior to deployment. The film

registered pressures exceeding 175 kg/cm^2 directly over areas that were injured. These injuries could not have been caused by fabric scraping because the plastic film protected the skin from scraping but not from normally directed impact.

High-speed films of deployments in the current test series showed that the most severe abrasions, those from tests with 400-kPa inflators and A folds, resulted from a fabric wing impact similar to those observed in the previous research (see Figure 13). Both the areas of injury and the areas of peak pressure were located at the point of initial contact of the fabric wing. Since the peak surface pressures were below those believed necessary to cause skin injury without shear, the current data suggest that abrasion can occur with pressures below 175 kg/cm^2 if lateral fabric motion is also present.

Figure 14 shows a schematic depiction of the proposed relationship between surface pressure, surface shear, and injury severity. The horizontal axis (not to scale) represents the peak surface pressure produced by airbag fabric contact. The vertical axis represents an unscaled shear produced by lateral fabric motion. This surface shear due to fabric friction is not independent of pressure, because higher pressure will allow higher shear force to be generated with the same fabric speed and roughness. Injury severity, as measured by the depth of the injury rather than the area, increases as either the surface pressure or shear are increased above certain threshold levels.

In the previous study, abrasions were seen both with shearing action (area C in Figure 14) and without shearing action (area D) when pressures exceeded 175 kg/cm^2. In the current study, a few injuries were observed at 275 mm (stamp-type abrasions produced without substantial shearing action) when pressures exceeded 90 kg/cm^2 (area B). However, most of the abrasions occurred at 200 mm in areas exceeding 90 kg/cm^2 when shearing due to fabric wing action was also present (area A). Thus, the 90-kg/cm^2 threshold level that was found to predict abrasion area fairly well in tests at 200 mm, where shear loading due to fabric wing motion was present, did not predict abrasion area at 275 mm, where shear was largely absent. Consistent with this analysis, the wing-type abrasions in the previous study, which involved both shear and high surface pressure, were more severe (deeper) than those in the current investigation.

Two important pressure values are those that mark the upper and lower range of pressures for which the presence of shear influences whether an abrasion will occur. The previous research indicated that abrasion can occur without fabric shear at pressure levels above about 175 kg/cm^2. Data from the current study show that injury can occur in areas where the Prescale pressure is between 90 kg/cm^2 and 175 kg/cm^2 when lateral fabric motion is also present. At some lower pressure level, abrasion would not occur even with high lateral fabric velocities, because the normal force would be insufficient to generate an injurious level of shear (frictional) force and the normal force would be well below the level sufficient to cause abrasion without shear (*i.e.*, about 175 kg/cm^2). Patterns in the Prescale-film images from near the areas of injury suggest that there are pressure levels within the range of the film that are low enough that the lateral fabric velocities produced in these tests did not cause abrasion. This lower-threshold pressure level is estimated to

be about 60 kg/cm^2, which is approximately the lower bound of the sensitivity range of the Prescale film.

It would be fairly difficult to separate the effects of the pressure generated at the point of impact and the lateral fabric motion because each is due to the motion of the airbag fabric. Impact pressure is correlated with fabric velocity for a particular airbag fabric, so adjusting the two factors independently would require changing the mass of the fabric. Given the complexity of airbag testing and the large kinematic variability inherent in airbag deployments, such an investigation would be difficult to conduct. In practice, accurate determination of this lower threshold is not expected to be critical because abrasions occurring near the lower threshold are not likely to be severe either in depth or area. Fold techniques that reduce lateral fabric motion during high-impact-velocity events have been demonstrated (*e.g.*, the B fold in this study). Engineering changes to reduce fabric impact pressures are also likely to reduce lateral fabric motions during impact events, contributing further to injury reduction.

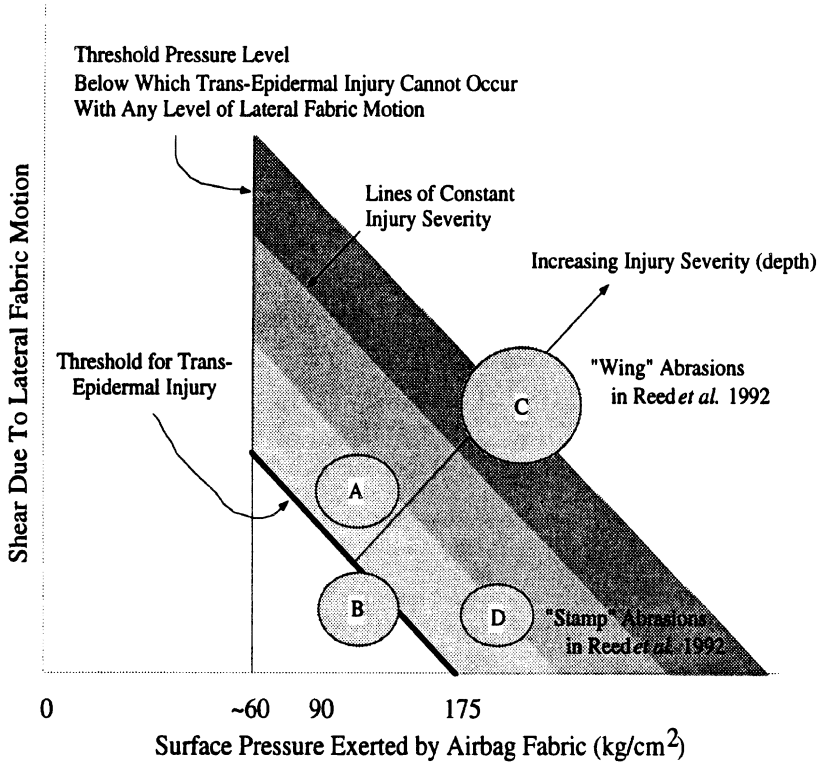

FIGURE 14. Schematic of proposed relationships among abrasion severity, surface pressure, and surface shear due to lateral fabric motion. See text for description of labeled areas.

4.3 APPLICATION OF STUDY FINDINGS

The findings of this study indicate that application of the Prescale-film technique for predicting airbag-induced skin abrasions is more complex than previously thought. A thorough analysis of airbag fabric kinematics, which had been recommended as a means

of selecting appropriate test conditions (Reed and Schneider 1993), is now regarded as an integral part of the abrasion-prediction procedure.

The test protocol described in Reed and Schneider (1993) has not been changed. Following testing, the Prescale film should be scanned and a scaled calibration curve generated using the methods described in Section 2.2.2. Pixel values corresponding to the 90- and 175-kg/cm^2 thresholds should be calculated for use in the analysis. The entire Prescale-film image should be analyzed, rather than the smaller region used in this study. Suitable software (*e.g.*, NIH Image) should be used to depict the Prescale image as a pressure map.

If areas of the pressure map exceed 175 kg/cm^2, abrasion is predicted regardless of the fabric action that produced the pressure peaks. This is most likely to occur from stamp-type actions with high-output inflators or from wing-type contacts between flaps of airbag fabric and the target surface. If pressures between 90 and 175 kg/cm^2 are observed, the fabric kinematics that produced the pressure peaks should be examined closely. If the pressures are at the low end of the range, and the fabric action appears to be primarily normally directed, then abrasion is not likely. In contrast, if the pressure is at the higher end of the range, or lateral fabric motion is also present, then abrasion is likely. Multiple tests in each condition should be conducted because of the known variability in the deployment characteristics affecting abrasion. Good practice would be to conduct repeated tests, calculating a running estimate of variance, until the predicted area of injury is estimated within a reasonable confidence range (*e.g.*, 100 mm^2). If the area in which the pressure exceeds 90 kg/cm^2 is small, and the fabric kinematics indicate a minimal amount of lateral fabric motion, then abrasion should be considered unlikely or of minimal severity, both with regard to depth and area.

Ultimately, judgments regarding the abrasion potential of airbag systems should be made with human-subject tests after careful evaluation with the Prescale-film procedure. Over 100 human-subject tests conducted at UMTRI have demonstrated the safety of human-subject testing when the test conditions are carefully controlled. Human testing should *not* be attempted until after Prescale testing has been conducted to estimate the potential for abrasion. This procedure was followed successfully in selecting test conditions for this study, using the previously defined guidelines. The new guidelines described in this report will result in even more accurate predictions.

5.0 CONCLUSIONS

1. Abrasion severity decreased with increasing distance from the module, consistent with previous investigations.

2. At 200 mm with 400-kPa inflators, the B fold produced less severe abrasions than the A fold. At 275 mm, there were no significant differences between the two folds because neither produced substantial abrasions.

3. Gender and the module cover factor were not found to have a significant effect on abrasion severity.

4. Investigations of a possible Inflator effect suggest that interlot variability in inflator output may influence abrasion severity. Tests investigating other factors should carefully control inflator output by using inflators from a single lot when possible.

5. Intersubject variability in skin sensitivity to abrasion was a substantial fraction of the total test-retest variance. The variance estimates in this report should be used in the design of future experiments.

6. The test-retest variance was also a substantial fraction of the range of the dependent variables, both for the human-subject and Prescale tests. This variability reduced the correlations between the two data sets. Greater correlations could be achieved by increasing the sample size, decreasing the variance due to airbag-related factors (*e.g.*, inflator output), or by increasing the range of injury severities. The latter is not regarded as an ethically acceptable means of obtaining a stronger correlation.

7. A significant correlation between Prescale(60) and injury data was observed for tests at 200 mm, but no correlation was apparent in data from 275 mm. This finding, coupled with an analysis of airbag fabric kinematics, suggests that abrasion can occur at pressures lower than the previously identified threshold of 175 kg/cm^2 in the presence of lateral fabric motion across the skin surface. The fact that abrasion only occurs in areas of relatively high pressure (at the point of initial fabric contact) and not in the entire area swept by the fabric indicates that the relatively high pressures caused by the fabric impact *are* necessary to cause abrasion, but, in the presence of scraping action, the critical pressure level may be considerably lower than previously thought, *e.g.*, 90 kg/cm^2 rather than 175 kg/cm^2.

8. Kinematic analysis should be an integral part of the Prescale-film test procedure. Abrasion is predicted by high surface pressures (greater than 175 g/cm^2), or lower pressures (90 kg/cm^2) in conjunction with lateral fabric motions. Confirmatory human-subject testing should complement the Prescale-film testing.

REFERENCES

Evans, L. (1990). Restraint effectiveness, occupant ejection from cars, and fatality reductions. *Accident Analysis and Prevention*, 22:167-175.

Huelke, D.F., Roberts, J.V., and Moore, J.L. (1993). Air bags in crashes: clinical studies from field investigations. *Proc. 13th International Technical Conference on Experimental Safety Vehicles,* pp. 140-148. U.S. Department of Transportation, National Highway Traffic Safety Administration, Washington, D.C.

Huelke, D.F., Moore, J.L., and Öström, M. (1992). Air bag injuries and occupant protection. *Journal of Trauma*, 33(6):894-898.

Kikuchi, A., Horii, M., Kawai, S., Komaki, Y., and Matsuno, M. (1975). Injury to eye and facial skin (rabbit) on impact with inflating air bag. *Proc. 2nd International Conference on the Biomechanics of Serious Trauma,* pp. 289-296. Edited by J.P. Cotte and M.M. Presle. IRCOBI, Bron, France.

Rasband, W. (1993). *NIH Image software, Version 1.52.* National Institutes of Health, Washington, D.C.

Reed, M.P., Schneider, L.W., and Burney, R.E. (1992). Investigation of airbag-induced skin abrasion. In *Proc. 36th Stapp Car Crash Conference*, pp. 1-12. Society of Automotive Engineers, Inc., Warrendale, PA.

Reed, M.P. and Schneider, L.W. (1993). *A laboratory technique for assessing the skin abrasion potential of airbags.* SAE Technical Paper 930644. Society of Automotive Engineers, Inc., Warrendale, PA.

Rimmer, S., Shuler, J.D. (1991). Severe ocular trauma from a driver's-side airbag [letter]. *Archives of Ophthalmology*, 109:774.

SAS Institute (1993). *JMP User's Guide. Version 2.* SAS Institute, Cary, NC.

Schneider, L., Johnson, G., Öström, M., Reed, M., Burney, R., and Flannagan, C. (1991). *Investigation of airbag-induced skin abrasions using deployments into human volunteers.* Final Report no. UMTRI-91-32. University of Michigan Transportation Research Institute, Ann Arbor.

APPENDIX A

POST-TEST PHOTOGRAPHS OF INJURIES

This appendix contains photos of the subjects' legs taken 15 minutes after deployment. In most of the photos, little or no injury is apparent because the injury areas are small and the depth is minimal, resulting in little bleeding. The captions indicate test number and test conditions. In the test-condition information, B* indicates airbags that were intended to be configured with A folds but were supplied with B folds. See text for additional explanation.

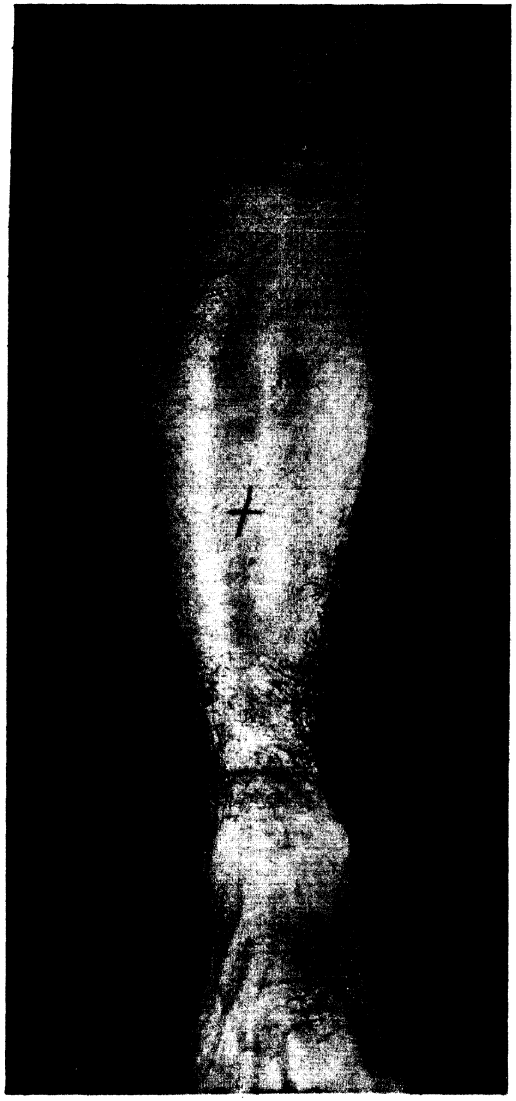

TA93015
350-kPa, B* Fold
200 mm, Unslit, Male

TA93016
350-kPa, B* Fold
200 mm, Unslit, Male

TA93019
350-kPa, B Fold
275 mm, Unslit, Male

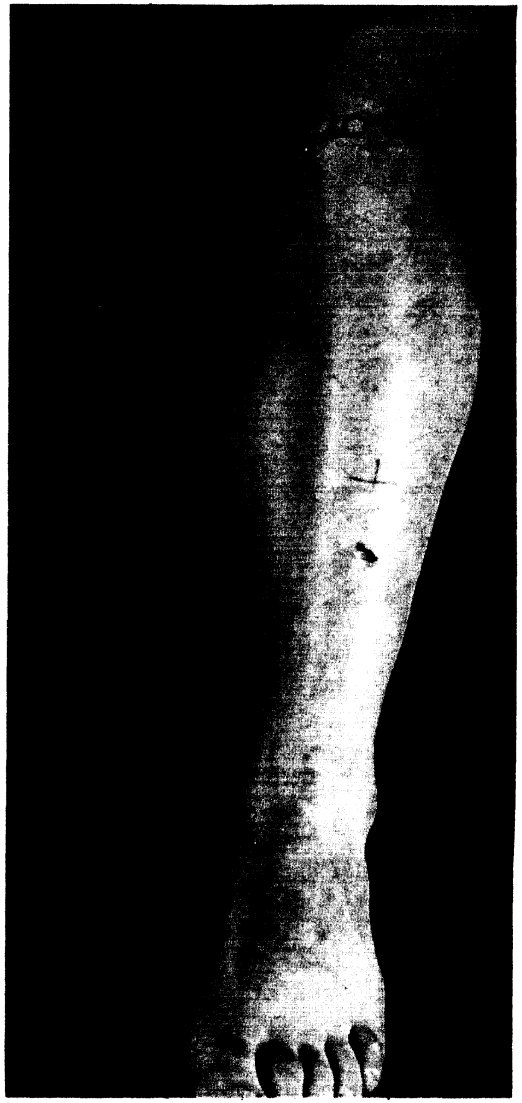

TA93020
350-kPa, B Fold
275 mm, Unslit, Male

TA93021
350-kPa, B Fold
200 mm, Slit, Male

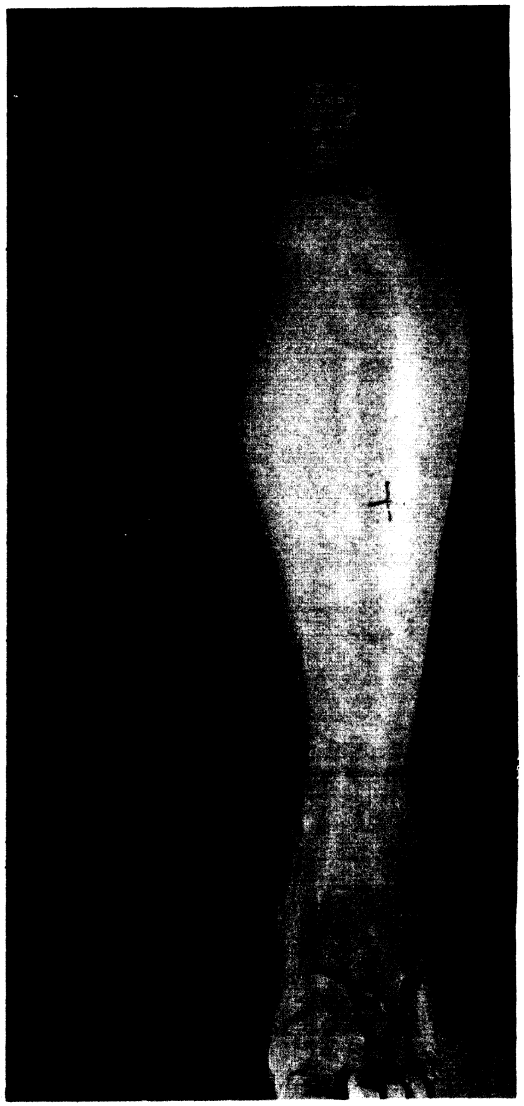

TA93022
400-kPa, B Fold
275 mm, Slit, Male

TA93023
350-kPa, B* Fold
200 mm, Slit, Female

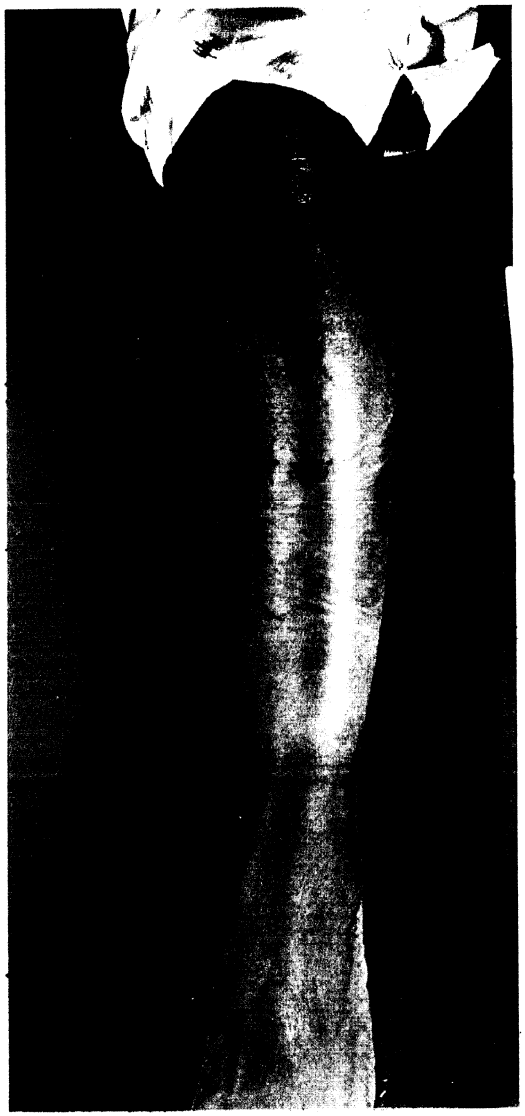

TA93024
350-kPa, B* Fold
200 mm, Slit, Female

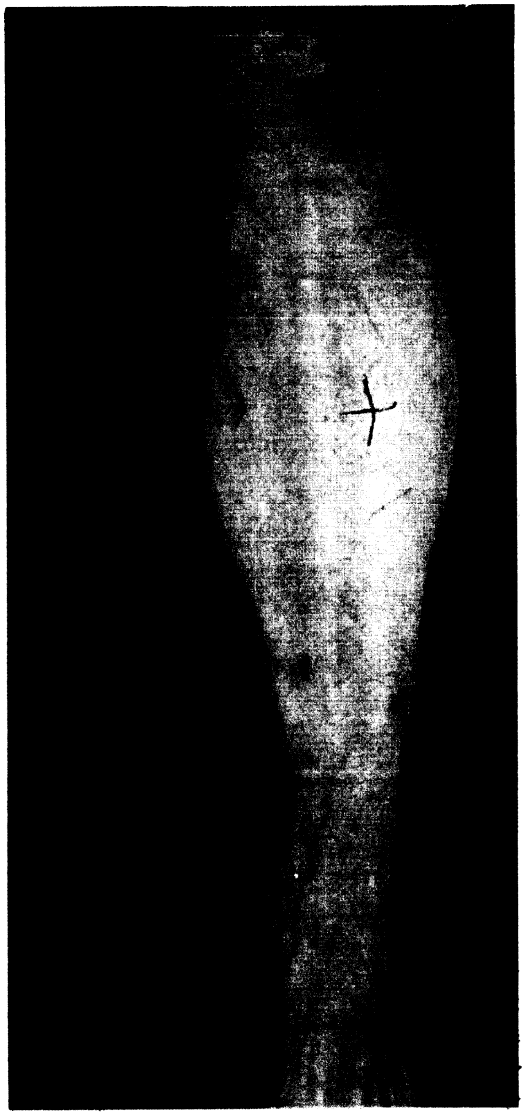

TA93025
400-kPa, B Fold
200 mm, Slit, Female

TA93026
400-kPa, B Fold
200 mm, Slit, Female

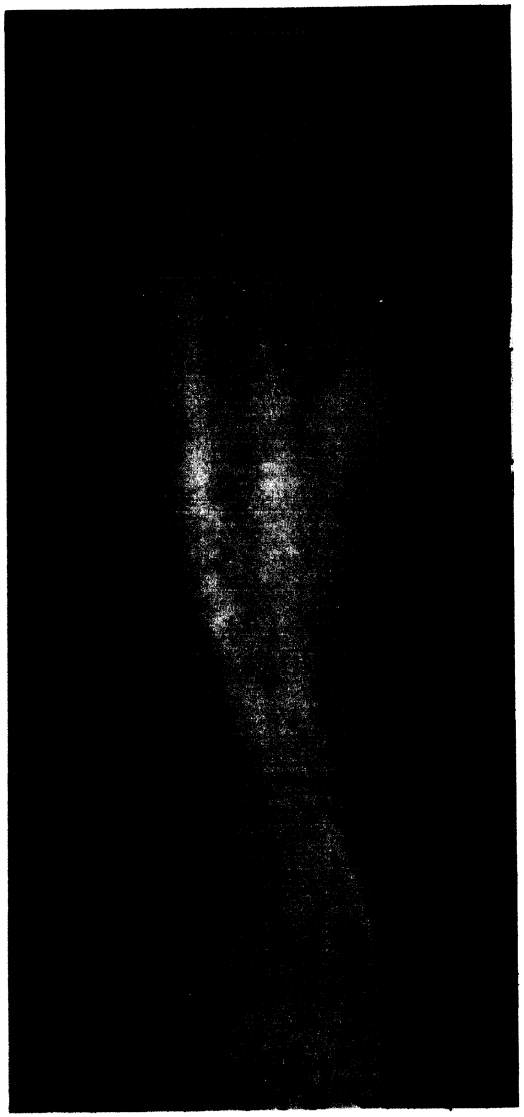

TA93027
350-kPa, B* Fold
275 mm, Slit, Female

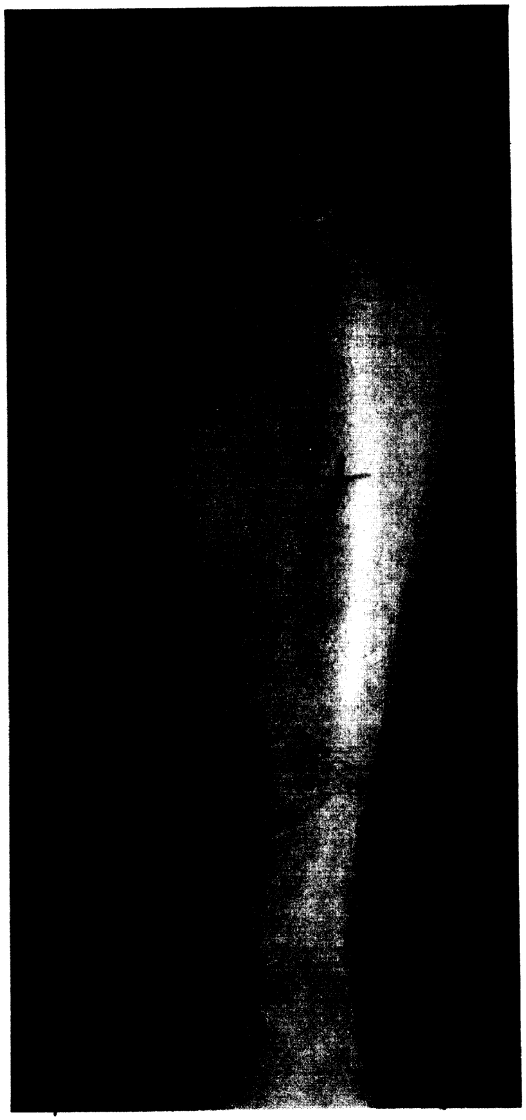

TA93028
350-kPa, B* Fold
275 mm, Slit, Female

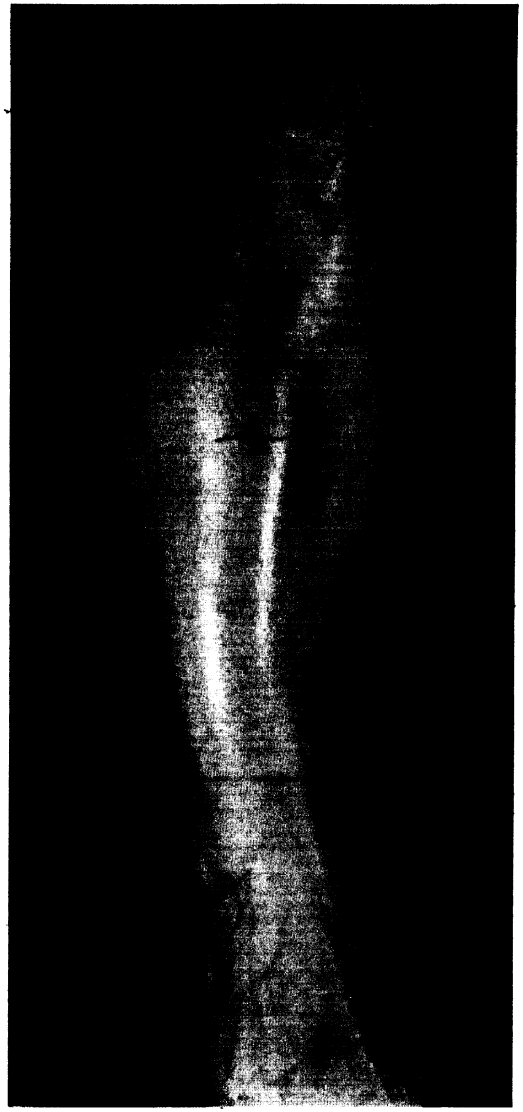

TA93029
400-kPa, A Fold
275 mm, Slit, Female

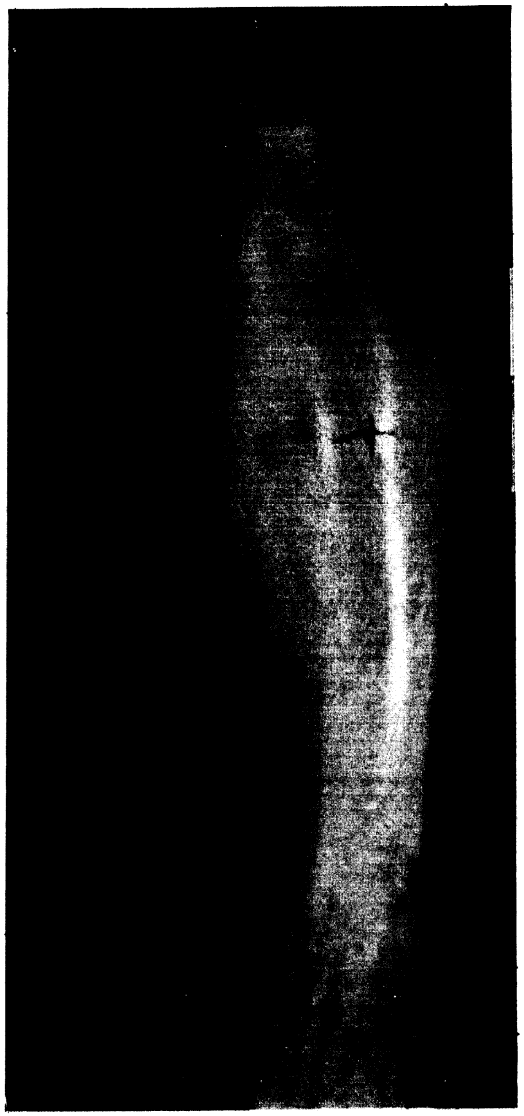

TA93030
400-kPa, A Fold
275 mm, Slit, Female

TA93031
400-kPa, B Fold
200 mm, Unslit, Male

TA93032
400-kPa, B Fold
200 mm, Unslit, Male

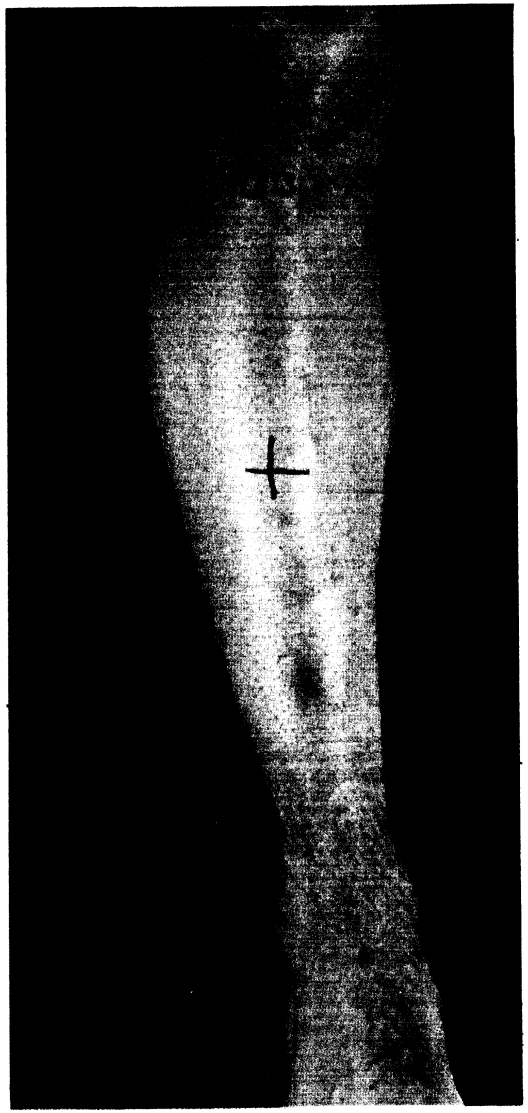

TA93033
400-kPa, A Fold
275 mm, Unslit, Male

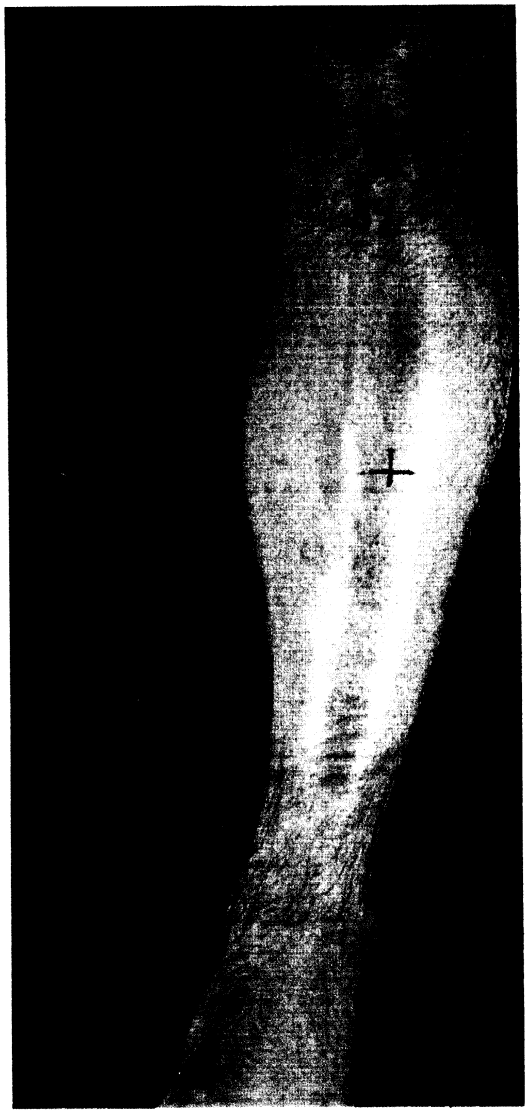

TA93034
400-kPa, A Fold
275 mm, Unslit, Male

TA93035
350-kPa, B Fold
200 mm, Unslit, Female

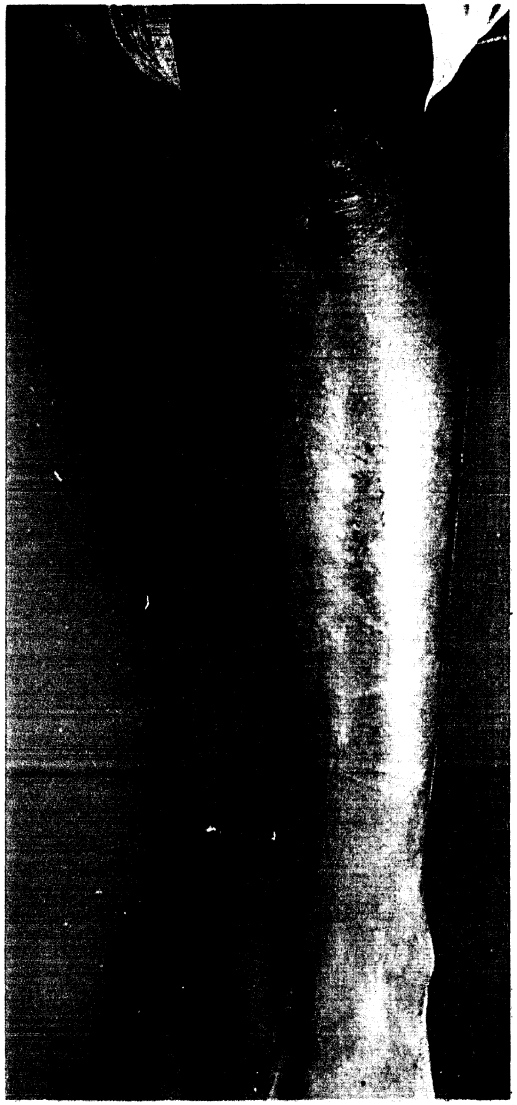

TA93036
400-kPa, B Fold
275 mm, Unslit, Female

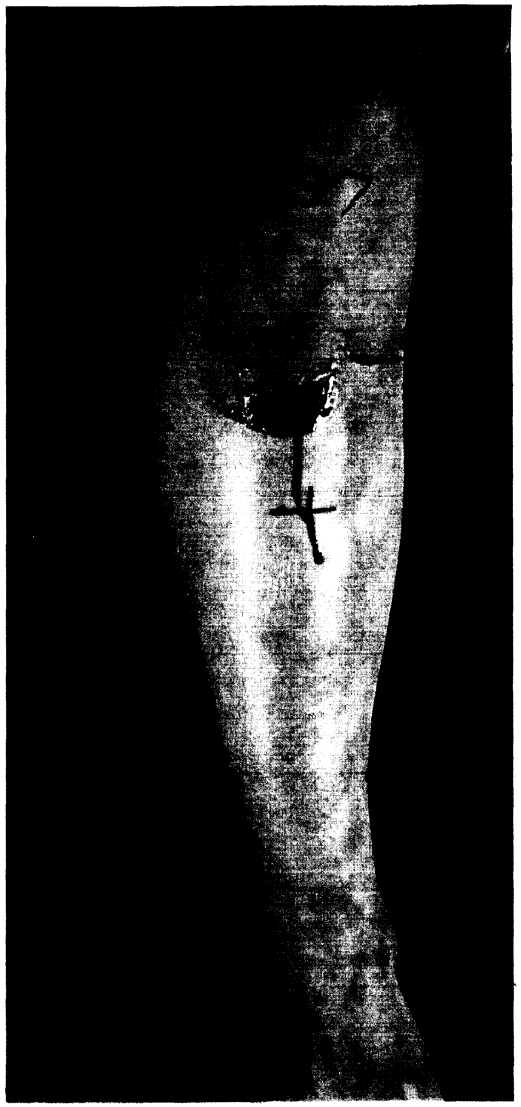

TA93037
400-kPa, A Fold
200 mm, Unslit, Female

TA93038
350-kPa, B Fold
200 mm, Unslit, Female

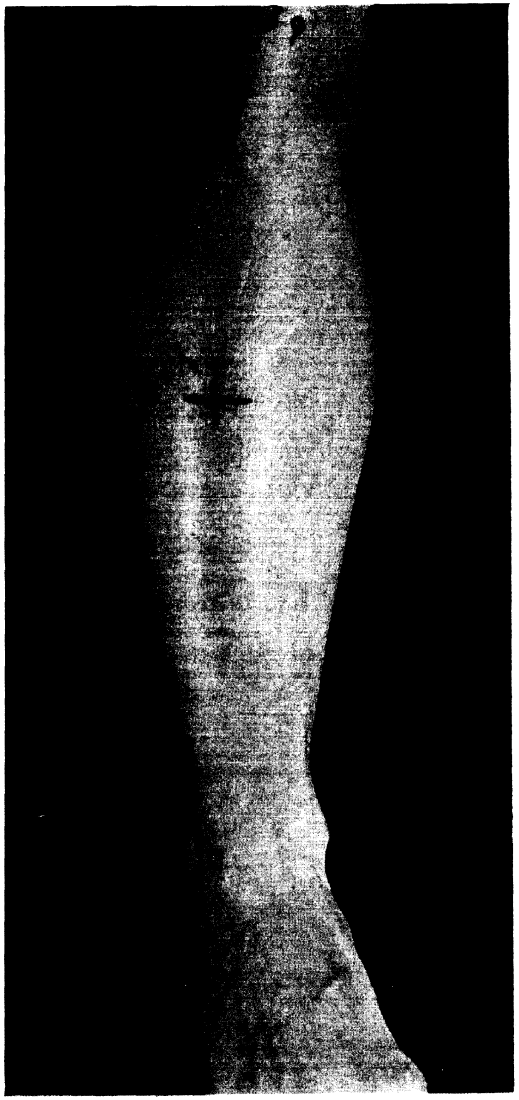

TA93039
350-kPa, A Fold
275 mm, Unslit, Female

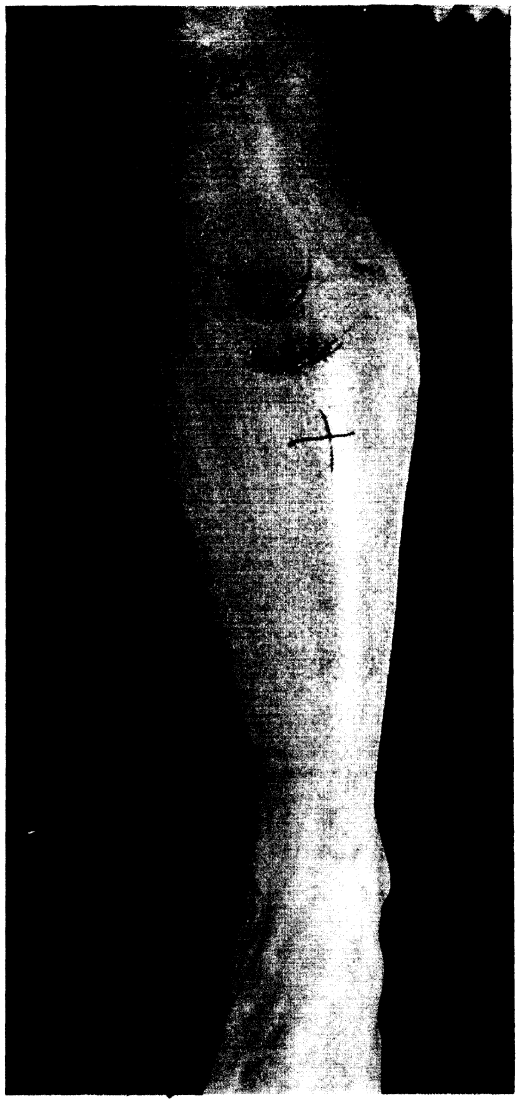

TA93040
400-kPa, A Fold
200 mm, Unslit, Female

TA93041
350-kPa, B Fold
200 mm, Slit, Male

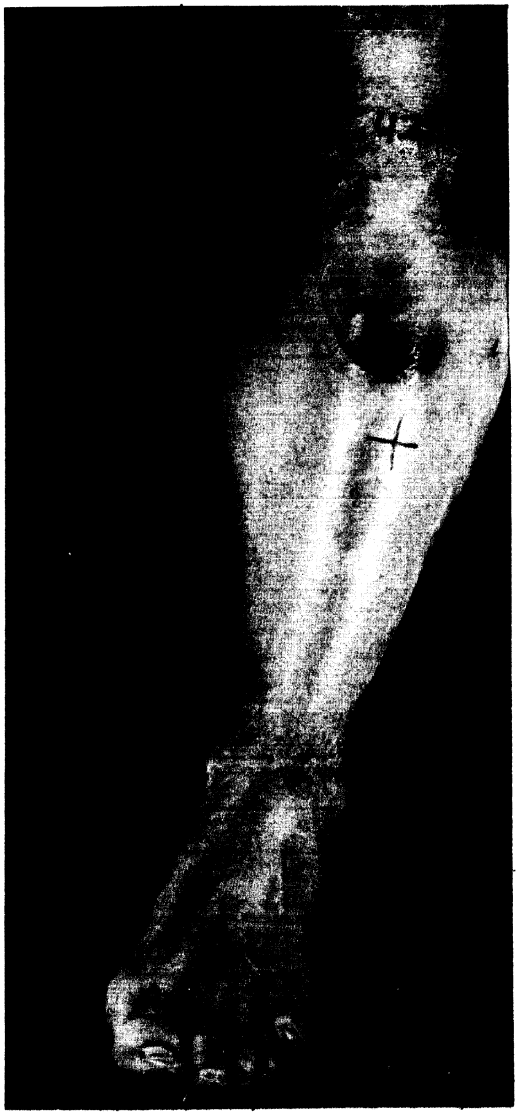

TA93042
400-kPa, A Fold
200 mm, Slit, Male

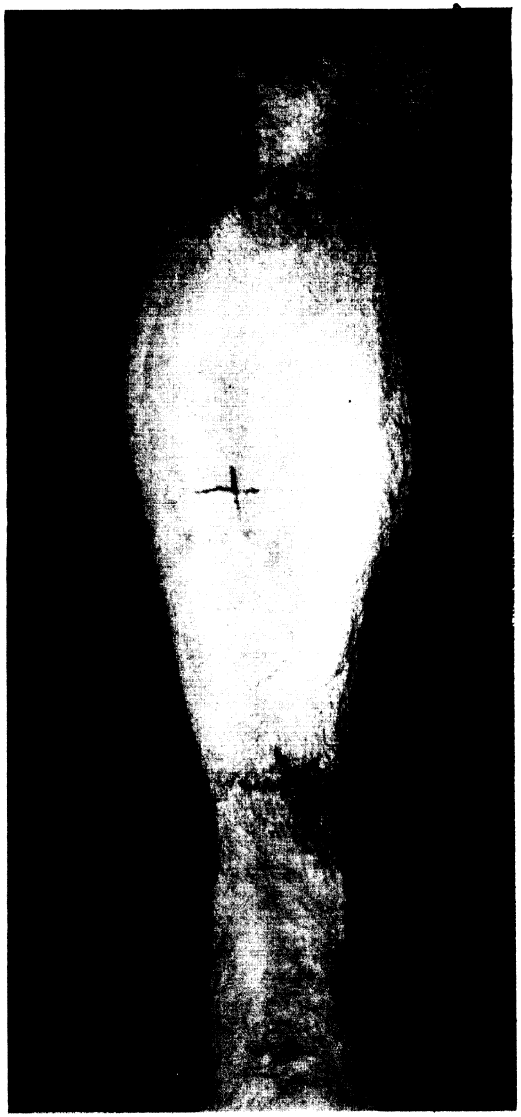

TA93043
350-kPa, A Fold
275 mm, Slit, Male

TA93044
400-kPa, A Fold
200 mm, Slit, Male

TA93045
350-kPa, B* Fold
275 mm, Slit, Male

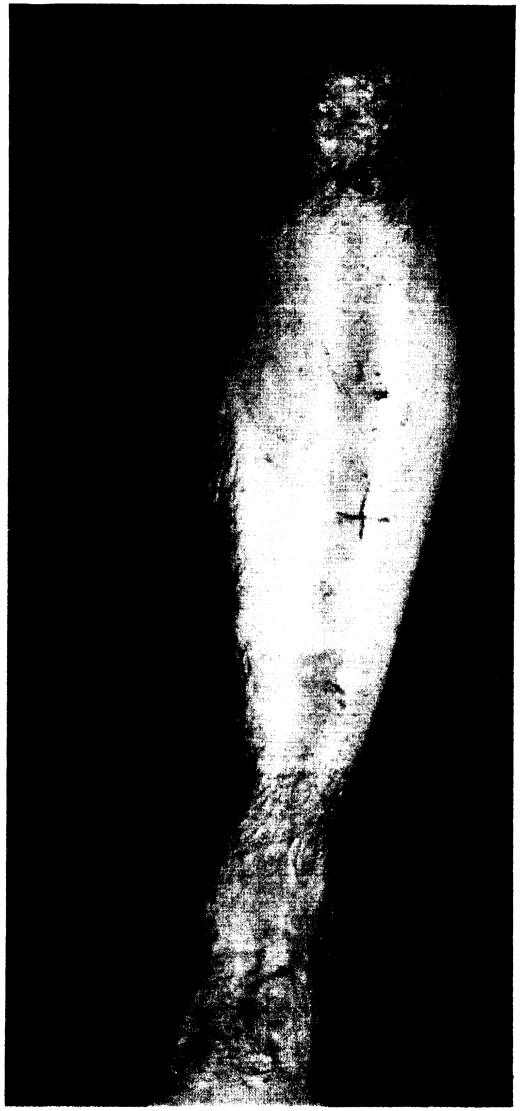

TA93046
400-kPa, B Fold
275 mm, Slit, Male

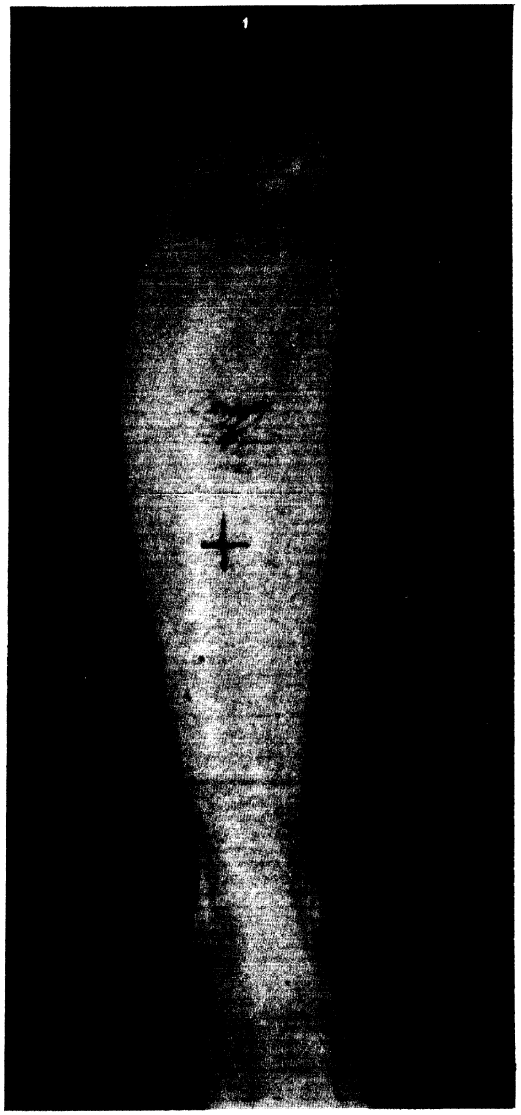

TA93047
350-kPa, B* Fold
275 mm, Unslit, Female

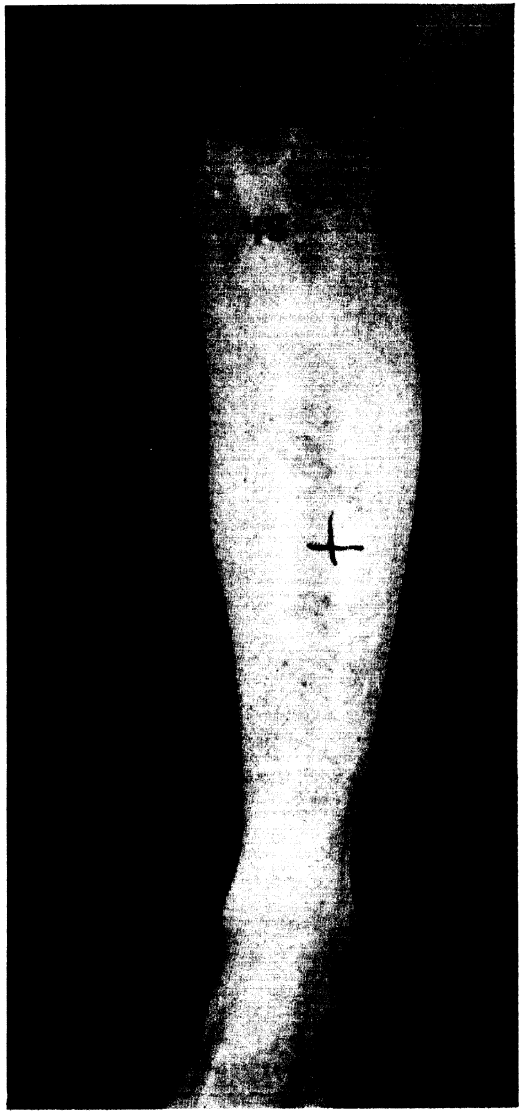

TA93048
400-kPa, B Fold
275 mm, Unslit, Female

APPENDIX B

DIGITAL SCANS OF PRESCALE IMAGES

This appendix contains the digitized Prescale images. The images were scanned in 8-bit grayscale at 75 dpi and printed on a 600-dpi laser printer. Test numbers and test conditions are summarized below each scan. The irregular white areas at the top of each scan are areas where hand-written test numbers were digitally erased. In the test-condition information, B* indicates airbags that were intended to be configured with A folds but were supplied with B folds. See text for additional explanation.

TA93049
350-kPa, B* Fold
200 mm, Slit Cover

TA93050
350-kPa, B* Fold
200 mm, Slit Cover

TA93051
350-kPa, B Fold
200 mm, Unslit Cover

TA93052
350-kPa, B Fold
200 mm, Unslit Cover

TA93053
400-kPa, A Fold
200 mm, Unslit Cover

TA93054
400-kPa, A Fold
200 mm, Unslit Cover

TA93055
400-kPa, B Fold
200 mm, Slit Cover

TA93056
400-kPa, B Fold
200 mm, Slit Cover

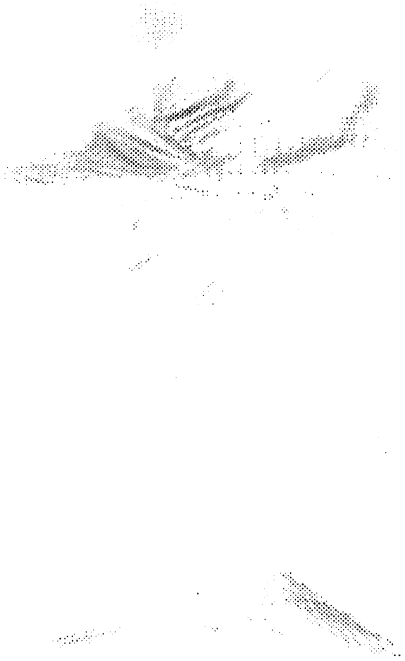

TA93057
350-kPa, B* Fold
200 mm, Unslit Cover

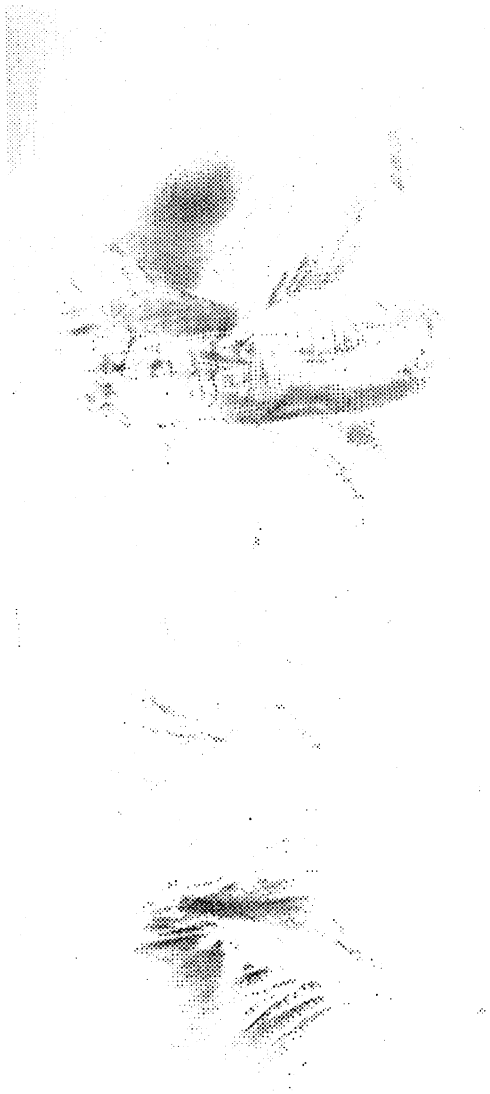

TA93058
350-kPa, B* Fold
200 mm, Unslit Cover

TA93059
350-kPa, B Fold
200 mm, Slit Cover

TA93060
350-kPa, B Fold
200 mm, Slit Cover

TA93061
400-kPa, A Fold
200 mm, Slit Cover

TA93062
400-kPa, A Fold
200 mm, Slit Cover

TA93063
400-kPa, B Fold
200 mm, Unslit Cover

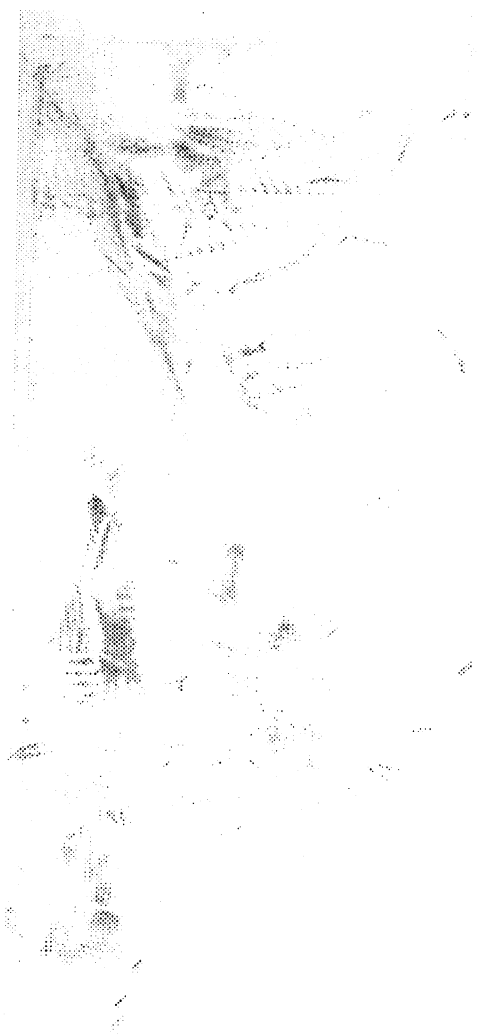

TA93064
400-kPa, B Fold
200 mm, Unslit Cover

TA93065
350-kPa, B* Fold
275 mm, Unslit Cover

TA93066
350-kPa, B* Fold
275 mm, Unslit Cover

TA93067
350-kPa, B Fold
275 mm, Slit Cover

TA93068
350-kPa, B Fold
275 mm, Slit Cover

TA93069
400-kPa, A Fold
275 mm, Slit Cover

TA93070
400-kPa, A Fold
275 mm, Slit Cover

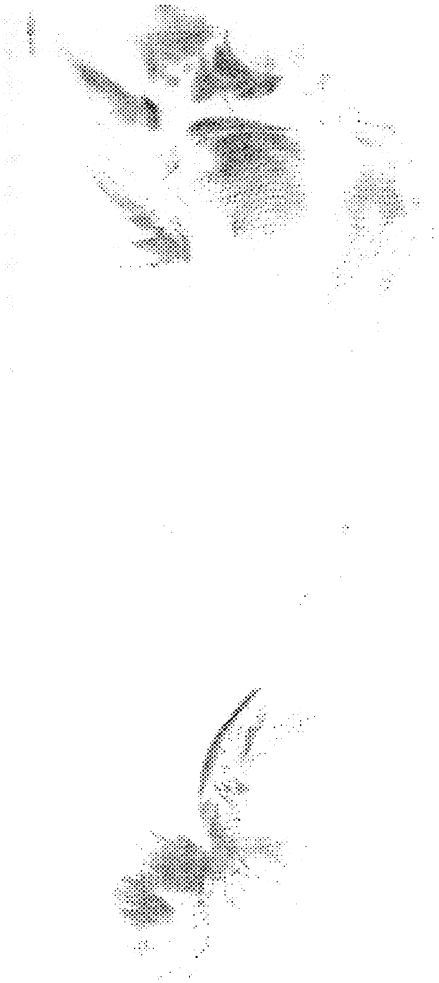

TA93071
400-kPa, B Fold
275 mm, Unslit Cover

TA93072
400-kPa, B Fold
275 mm, Unslit Cover

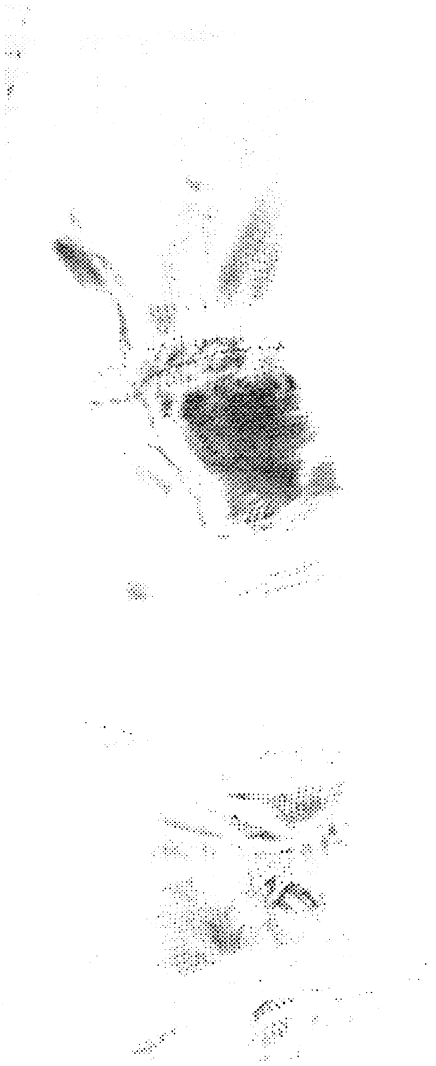

TA93073
350-kPa, B* Fold
275 mm, Slit Cover

TA93074
350-kPa, B* Fold
275 mm, Slit Cover

TA93075
350-kPa, B Fold
275 mm, Unslit Cover

TA93076
350-kPa, B Fold
275 mm, Unslit Cover

TA93077
400-kPa, A Fold
275 mm, Unslit Cover

TA93078
400-kPa, A Fold
275 mm, Unslit Cover

TA93080
400-kPa, B Fold
275 mm, Slit Cover

TA93079
400-kPa, B Fold
275 mm, Slit Cover